

National Transportation Safety Board

Office of Research and Engineering

Washington, DC 20594



WPR23FA034

AIRCRAFT PERFORMANCE & SIMULATION STUDY

by John O'Callaghan

April 11, 2024

TABLE OF CONTENTS

A. ACCIDENT3

B. AIRCRAFT PERFORMANCE GROUP3

C. SUMMARY3

 C.1. Introduction3

 C.2. Objective and scope of the *Aircraft Performance & Simulation Study*4

 C.3. Summary of results5

D. DETAILS OF THE INVESTIGATION8

 D.1. The Cessna 208B Grand Caravan EX airplane8

 D.2. Wreckage location and condition9

 D.3. Automatic Dependent Surveillance - Broadcast (ADS-B) data 10

 D.3.1. Overview 10

 D.3.2. Calculation of additional performance parameters from ADS-B data 11

 D.4. Radar data 12

 D.4.1. Description of ARSR and ASR radar data 12

 D.4.2. Primary and secondary radar returns 13

 D.4.3. Recorded radar data 14

 D.5. Pratt & Whitney FAST engine monitoring data 15

 D.6. Simulation of the approach to stall and stall departure 16

 D.6.1. Simulation description and assumptions 16

 D.6.2. Simulation results 17

 D.7. Stall characteristics testing and upset recovery guidance 20

 D.7.1. Upset recovery guidance in the FAA *Airplane Flying Handbook* 20

 D.7.2. FAA stall characteristics certification standards and flight test guidance 23

 D.7.3. Risk mitigation in the *Test Plan* and the *Flight Test Safety Database* 26

 D.7.4. Stall and overspeed guidance in the 208B POH and Maintenance Manual 28

 D.7.5. Additional upset recovery guidance 30

E. CONCLUSIONS 31

F. REFERENCES 34

G. GLOSSARY 35

FIGURES 37

A. ACCIDENT

Location: Snohomish, Washington
Date: November 18, 2022
Time: 10:19 Pacific Standard Time (PST)
18:19 Coordinated Universal Time (UTC)
Airplane: Textron Aviation 208B Grand Caravan EX, N2069B

B. AIRCRAFT PERFORMANCE GROUP

Chairman: John O'Callaghan
National Transportation Safety Board (NTSB), RE-60
Washington, D.C.

Members: N/A

C. SUMMARY

C.1. Introduction

On November 18, 2022, at 10:19 PST, a Textron Aviation¹ (Textron) 208B Grand Caravan EX, N2069B, was destroyed following an in-flight structural failure near Snohomish, Washington. All four occupants were fatally injured. The airplane was operated as a Title 14 Code of Federal Regulations Part 91 test flight.

The operator, Raisbeck Engineering (Raisbeck), holds the Supplemental Type Certificate (STC) for an aerodynamic drag reduction system (DRS) on the Cessna 208B Grand Caravan. The accident flight was part of the testing for Raisbeck to expand the applicability of that DRS to the Cessna 208B Grand Caravan EX model modified with the Aircraft Payload Extender (APE III) STC developed by AeroAcoustics Aircraft Systems Inc. QuickSilver Aero was contracted to provide instrumentation support for Raisbeck's flight test program. At the time of the accident, the Raisbeck DRS STC was not installed.

The airplane began flights to support the flight-test three days before the accident. The flights on the first day, consisting of three flights, totaled 1.1 hours and included a pilot familiarity flight and a ferry flight to have the airplane's weight and balance performed. Two days before the accident, the flight-test data-collection flights (establishing

¹ The Cessna Aircraft Company was acquired by Textron in 1992, and the Type Certificate for its 208B model was transferred to Textron in 2015. N2069B was manufactured in 2021, and consequently is Textron airplane; however, the manuals, STCs and simulation models referenced in this *Study* often refer to the "Cessna" 208B. The names of both companies are used equivalently throughout this *Study*.

baseline data) began. Those included two flights, totaling 4.6 hours of flight time, which were conducted to gather baseline data for both mid center-of-gravity (CG) cruise flight and forward CG stall speeds. The day prior to the accident, two test flights were performed with the accident test-pilot and the accident aft-seated testing personnel (different right-seated pilot). The first flight, totaling 1.2 hours, tested aft CG static stability. The last flight that day ended early, totaling 1.4 hours, with only about half of the test plan (card) completed because an aft crewmember was feeling airsick.

The purpose of the accident flight was to complete the tests specified on the prior day's test card, consisting of baseline testing of the aft CG stall characteristics of the airplane modified with the APE III STC. Witnesses reported that they observed the airplane break-up inflight and watched pieces floating down. The airplane then descended in a nose-low near-vertical corkscrew maneuver toward the ground (see Figure 1). Several witnesses reported seeing a white plume of smoke when they observed the airplane break into pieces. A security camera recorded a low-quality image of the airplane rotating about its longitudinal axis in nose-low attitude (see Figure 1).

Automatic Dependent Surveillance - Broadcast (ADS-B) and radar surveillance data for the flight indicates that after departing Renton, Washington around 09:25, the airplane flew north. The airplane gradually climbed to about 9,500 ft. mean sea level (MSL) and began a series of turns/maneuvers. The airplane maneuvered for about 45 minutes varying in altitude between about 6,500 ft. to 10,275 ft. MSL. The surveillance data indicates that at 10:17:00 the airplane was in a shallow left turn at an altitude of about 10,000 ft MSL (see Figure 2). The data further shows that between 10:17:40 and 10:19:00 the airplane made a 360° left turn and then, at 10:19:06, turned sharply 180° left (reversing course). The airplane's track continued west until the last ADS-B data point at 10:19:18. The last 12 seconds of the track indicated that the airplane's descent rate exceeded 14,000 ft./min., slowing to 8,700 ft./min. at the last ADS-B point. The main wreckage was located about 2,145 ft. west of that point. The accident site was located in a grass field in the rural farm land of Snohomish, about 2 nm east of Harvey Airfield, at about 0 ft. elevation.

C.2. Objective and scope of the *Aircraft Performance & Simulation Study*

The objective of this *Aircraft Performance & Simulation Study* is to determine and analyze the motion of the airplane and the physical forces that produce that motion. In particular, the *Study* attempts to define the airplane's position and orientation during the relevant portion of the flight, and determine the airplane's response to control inputs, external disturbances, and other factors that could affect its trajectory.

The data used to determine and analyze the airplane motion includes the following:

- Air Traffic Control (ATC) surveillance data (both ADS-B and radar).

- Data recorded on a Pratt & Whitney (P&W) Full Flight Data Acquisition, Storage, and Transmission (FAST) engine monitoring device.
- Wreckage location and debris field evidence.
- Weather information, including winds aloft.
- Airplane performance information in the Pilot's Operating Handbook (POH).
- Output from aircraft performance analysis programs and simulations.
- Flight test cards and test plans provided by Raisbeck.

N2069B was not equipped (and was not required to be equipped) with a Flight Data Recorder (FDR) or Cockpit Voice Recorder (CVR), though it was equipped with a flight-test data acquisition system as part of its flight-test program. However, the data recording devices on the airplane were destroyed in the accident and no flight-test data for the accident flight was recovered.

N2069B was also equipped with a P&W FAST engine monitoring system. According to the P&W web page describing this system,²

Our FAST™ digital engine health management solution captures, analyzes and wirelessly sends full-flight data intelligence to you within minutes of engine shutdown so you can maximize aircraft availability, optimize maintenance planning, and reduce operating costs.

Recorded engine and other data from the FAST system was recovered from the wreckage and is presented below.

In this *Study*, the information listed above is used to define the trajectory of N2069B throughout its maneuvers during its last minutes of flight and sudden left turn and dive from 9,700 ft. MSL. An NTSB simulation incorporating aerodynamic, flight controls, and engine models of the Cessna 208B provided by Kohlman Systems Research (KSR) is then used to find a set of simulator flight control and throttle inputs that result in a simulated trajectory that approximately matches the trajectory defined by the recorded data.

C.3. Summary of results

The combination of ADS-B and winds-aloft data indicates that at 10:17:00 PST³, N2069B was flying in an approximately level, 10° left-banked turn at 10,000 ft. MSL and

² See <https://www.prattwhitney.com/en/services/pwc-engine-services/digital-engine-health-management/fast-solution>.

³ All times in this *Study* are in PST unless otherwise noted.

approximately 110 knots calibrated airspeed (KCAS) (see Figures 2, 10, and 11).⁴ At about 10:17:20, the airplane climbed to about 10,100 ft. MSL while slowing to between 90 and 105 KCAS. Shortly after 10:17:20, the left roll started to gradually but steadily increase, reaching 30° left at 10:18:38. At 10:17:50, the altitude started to decrease steadily at about 400 ft./min. from 9,700 ft. MSL, reaching 9,350 ft. MSL at 10:18:46. The airspeed remained approximately constant at 105 KCAS between 10:18:20 and 10:18:44. Between 10:16:50 and 10:19:05, the FAST data shows the engine torque constant at about 930 ft.-lb., after which it increased abruptly, reaching about 2,200 ft.-lb. at 10:19:20.

At 10:18:43, the computed airspeed started to drop relatively quickly from 105 KCAS, reaching a minimum of 48 KCAS at 10:19:01 before increasing rapidly. The indicated airspeed recorded by the FAST was 35 knots indicated airspeed (KIAS) at 10:19:00, and 37 KIAS at 10:19:03. The FAST indicated airspeed then also increased rapidly, reaching a maximum of 223 KIAS at 10:19:21, before dropping precipitously to approximately 80 KIAS as the airplane descended to the ground.

Between 10:18:47 and 10:18:59, as the airspeed was dropping, the altitude climbed from 9,320 ft. to 9,680 ft. MSL, after which it started to decrease. The vertical speed decreased from +2,560 ft./min. at 10:18:54 to -14,000 ft./min. at 10:19:13; between 10:19:25 and the end of the FAST data at 10:19:52, the average vertical speed computed from the FAST pressure altitude data was about -12,000 ft./min.

At 10:19:05, the ADS-B data shows a very sudden and tight course reversal from east to west. This is near the time of minimum airspeed and the dramatic increase in the rate of descent. From 10:18:44 up until this course reversal, the computed roll angle is approximately constant at about 30° left.

The ADS-B data ends at 10:19:17.5, at an altitude of about 7,400 ft. MSL, and a recorded descent rate of 8,700 ft./min. The location of the accident site about 0.18 nm west of the last ADS-B and radar returns, and the appearance of a “cloud” of primary radar targets over and west of the accident site (see Figure 3), indicate that N2069B likely broke apart in mid-air shortly after the last ADS-B return (consistent with the evidence at the wreckage site, witness statements, and the video images in Figure 1). The FAST data continued to record past the time of the last ADS-B return, and was evidently recording even after the airplane broke apart. The last FAST data point was recorded at 10:19:51.9, at a pressure altitude of 88 ft. MSL.

⁴ Several Figures in this *Study* have an “a” and a “b” version, which present the same information but at different scales, or with different background images. When the *Study* refers to a Figure with two or more versions without specifying the version, all versions are meant to be included in the reference.

The airplane behavior described above leading up to the time of minimum airspeed at about 10:19:01 is consistent with the execution of an intentional stall in a 30° left roll, with the engine power above idle (at about 930 ft.-lb. of torque). The execution of such a maneuver is itself consistent with the stated intent of the flight (baseline testing of the airplane's aft-CG stall characteristics) and the items remaining on the flight-test card for that flight (including a power-on stall in a 30° bank).

The sudden course reversal at about 10:19:05 indicates that following the stall-break, the airplane rolled further to the left. A simulation of the maneuver that roughly matches the track of the airplane indicates that the roll angle might have reached -120°, and that the pitch angle dropped to between -53° and -62°. The FAST data indicates that following the stall the engine torque increased from about 930 ft.-lb. to over 2,200 ft.-lb. The FAST airspeed peaked at 223 KIAS about 3 seconds after the end of the ADS-B data before dropping precipitously, suggesting that the airplane broke apart at or shortly before this time.

A simulation of the Cessna 208B was used to determine flight control and throttle inputs that result in an approximate "match" of the ADS-B, winds-aloft, and FAST torque data. A "match" results when the differences between the trajectory (position, speed, and attitude) of the simulated airplane and the trajectory computed from the ADS-B and winds-aloft data are smaller than desired tolerances. Unlike the tolerances defined in 14 Code of Federal Regulations (CFR) Part 60 for the qualification of pilot training simulators, the "desired tolerances" for this exercise are not precisely defined or rigorous. Uncertainties and errors associated with the simulation models, recorded data, winds, and computed airplane state have to be considered, so that determining whether the simulation results are reasonably representative of the recorded data, and can provide insight into airplane performance parameters that are not recorded (or into other circumstances of the accident), is largely a matter of engineering judgement. In this *Study*, comprehensive plots comparing the simulator results with the recorded data are provided to facilitate such judgement.

The simulation results were obtained by progressively lowering the flaps from 0° at 10:17:20 to 26.6° (the maximum flap setting in the simulation aerodynamic model) at 10:17:43.5. The maximum lift coefficients (C_{Lmax}) computed from the ADS-B and winds aloft data and obtained in the simulation are most consistent with the stall occurring at full flaps, and according to Reference 8, N2069B's flap motor/actuator was found in the full down position. Furthermore, a comparison of the airplane's maneuvers (as recorded in the ADS-B data) with the test cards intended for the flight, performed by the Raisbeck pilot who had flown in the airplane the day prior to the accident,⁵ suggests that the test crew were executing test condition "5.80L" (accelerated stall with a 30° left

⁵ Per an email from the NTSB Investigator In Charge dated 12/15/2022.

bank at landing flaps and 930 ft.-lb. torque) at the time of the accident. Consequently, it is likely that the flaps were fully down at the time of the stall break.

Per the *Cessna 208B Grand Caravan EX Pilot's Operating Handbook* (POH, Reference 1), the airplane's maximum operating speed (V_{MO}) is 175 KIAS, and the maximum flaps extended speed with landing flaps (V_{FE}) is 125 KIAS. Consequently, the FAST recorded airspeed of 223 KIAS at 10:19:21 was 98 KIAS above V_{FE} and 48 KIAS above V_{MO} . It is possible that the 223 KIAS data point is the result of airflow disruptions over the airplane's static pressure ports and / or pitot tube immediately following the airplane's structural failure, and therefore not an accurate measure of airspeed; the preceding data point (3 seconds earlier) recorded 200 KIAS, which exceeds V_{FE} and V_{MO} by 75 and 25 KIAS, respectively.⁶ In any case, the structural failure that likely occurred at about this time is consistent with these exceedances.

The sections that follow present the data used in this *Study* (as listed above), and describe the calculation of additional performance information from this data. The simulation model is also described, as are the methods used to match the available flight data with the simulation (note that the simulation presents only one of perhaps several possibilities for achieving a trajectory consistent with both the ADS-B data and the airplane's capabilities). The results of the performance calculations and simulation are presented in the Figures and Tables described throughout the *Study*.

D. DETAILS OF THE INVESTIGATION

D.1. The Textron Aviation 208B Grand Caravan EX airplane

The Textron Aviation 208B Grand Caravan EX (208B EX) is a fixed-gear, high-wing airplane powered by an 867 SHP Pratt and Whitney PT6A-140 turboprop engine, with a maximum takeoff weight of 8,807 lbs. N2069B was manufactured in 2021 (per FAA registration records), and was configured with seating for the pilot, co-pilot, test director, and instrumentation lead. The airplane also had test instrumentation equipment installed in the cabin, and was equipped with a belly cargo pod.

N2069B had been modified with AeroAcoustics Aircraft Systems Inc. STC #SA01213SE - Aircraft Payload Extender (APE) III, which added a stall fence on each wing leading edge, a scalloped gurney-type tab on each flap trailing edge, and high-cycle main

⁶ The certified dive speed (V_D) of the 208B EX is 240 KIAS. Per 14 CFR 23.251, in the cruise (flaps up) configuration "there must be no vibration or buffeting severe enough to result in structural damage, and each part of the airplane must be free from excessive vibration, under any appropriate speed and power conditions up to V_D/MD ."

landing gear axles. The STC increased the maximum landing and takeoff weights to 9,000 lbs. and 9,062 lbs., respectively.

Figure 4 is a pre-accident and pre-APE III STC photograph of N2069B. Figure 5 shows three-view diagrams of the 208B, taken from Reference 1. Raisbeck's weight and balance form for the accident flight (test flight 69B-008) is shown in Figure 6, and Figure 7 presents Raisbeck's flight test card for flight 69B-008. The predicted weight for condition 5.80L, the condition likely being executed at the time of the accident⁷, is shown in Figure 7 as 7,965 lb. This weight, and a center of gravity (CG) location at Fuselage Station (FS) 203.5 inches, are used in the performance calculations and simulation described in this *Study*.

As noted above, the purpose of Raisbeck's flight test campaign using N2069B was to expand the applicability of their DRS STC (which was not installed at the time of the accident) to the Cessna 208B Grand Caravan EX model with the APE III STC installed. The major difference between the Grand Caravan and the Grand Caravan EX is the increase in engine power from 675 SHP on the former to 867 SHP on the latter.

D.2. Wreckage location and condition

According to the NTSB preliminary report of the accident (Reference 2), the main wreckage, consisting of the engine, cockpit, cargo pod, cabin, vertical stabilizer, and rudder, was located in a grass field at the following coordinates:

47° 54' 21.4272" N latitude / 122° 02' 56.1120" W longitude

Per *Google Earth*, the elevation at these coordinates is 8 ft. MSL. The east and north coordinates of N2069B's flight path presented in Figures 2 and 3 are relative to the main wreckage site. The ADS-B and radar coordinates are converted from latitude and longitude into east and north coordinates from the accident site using the WGS84 ellipsoid model of the Earth.

Reference 2 notes that the wreckage was distributed over approximately 1,830 ft. on a median magnetic bearing of about 270°. The main wreckage and right wing were

⁷ Condition 5.80L should not be confused with condition 5.8L (the first item on the test card in Figure 7). Condition 5.8L has a target deceleration of -1 kt./sec., whereas condition 5.80L is an "accelerated" stall with a target deceleration of -3 to -5 kt./sec.

located at the beginning of the debris field, with the right wing about 580 ft north of the main wreckage. The right-wing strut separated from the fuselage attachment point but remained attached to the wing, and the right flap was separated into numerous pieces and scattered among the debris field. The left-wing separated from the fuselage but was located adjacent to the main wreckage. The left flap remained attached and was found in the retracted position, but Reference 8 adds that the flap motor/actuator was found in the full-down/LAND position.

As noted above, the computed C_{Lmax} achieved during the flight is most consistent with that corresponding to flaps in the fully deployed (landing) position at the time of the stall break.

D.3. Automatic Dependent Surveillance - Broadcast (ADS-B) data

D.3.1. Overview

N2069B was tracked by Air Traffic Control, using both ground-based radar and the Global Navigation Satellite System (GNSS)-based ADS-B system. Since the GNSS positions recorded in the ADS-B data are more accurate and frequent than radar data, only the ADS-B data are used to determine N2069B's position in this *Study*, though the ADS-B data are compared to data from several radar sources in Figure 3. The primary radar returns shown in Figure 3 are additional evidence of the in-flight breakup of the airplane. The radar data are described further in Section D.4.

ADS-B capability enables aircraft to broadcast their three-dimensional position (latitude, longitude, and altitude) to other ADS-B equipped aircraft and to ADS-B ground stations.⁸ ADS-B data broadcast from N2069B was received and recorded by Federal Aviation Administration (FAA) ADS-B ground stations.

ADS-B latitude and longitude are determined using GNSS signals, including those from Global Positioning System (GPS) satellites, and altitudes determined both barometrically and by GNSS are included in ADS-B messages. The GNSS positions are very accurate compared to radar data; radar range uncertainty alone (without even considering azimuth uncertainty) is about $\pm 1/16$ nm, or ± 380 ft., and GNSS positions are generally accurate to within 60 ft. (see Reference 3). Furthermore, ADS-B data are available at a higher frequency than radar data: typically at 1 sample/second for ADS-B, and at best, 1 sample every 4.5 seconds for radar.

The recorded ADS-B data includes the following parameters:

⁸ For more information about ADS-B, see https://www.faa.gov/air_traffic/technology/adsb.

- UTC time of the ADS-B report, in hours, minutes, and seconds. PST = UTC - 8 hours.
- Aircraft identifying information.
- Latitude and longitude, to a resolution of 0.01 arc-seconds (≈ 1 ft.)
- Pressure altitude in feet, to the nearest 25 ft. (an uncertainty band of ± 12.5 ft.)
- Geometric (GNSS) altitude in feet, to the nearest 25 ft. The GNSS altitude is the height above the WGS84 ellipsoid, which differs from MSL altitude by the height of the geoid.⁹ At the accident site, 72 ft. should be added to GNSS altitude to give MSL altitude.¹⁰
- North-south and east-west components of ground speed, to a resolution of 1 kt.
- Rate of climb, to a resolution of 1 ft./min.
- Numerous parameters documenting the quality and accuracy of each reported GNSS position.

The ADS-B data is presented in Figures 2, 3, 8, 9, and 10. Additional performance parameters, such as airspeeds and the airplane's Euler angles (pitch, roll, and heading) can be computed from the ADS-B data, as described below.

D.3.2. Calculation of additional performance parameters from ADS-B data

To calculate performance parameters (such as ground speed, track angle, pitch and roll angles, etc.) from surveillance data, it is convenient to express the position of the airplane in rectangular Cartesian coordinates. The Cartesian coordinate system used here is centered on the main wreckage coordinates specified in section D.2, and its axes extend east, north, and up from the center of the Earth. The ADS-B data are converted into this coordinate system using the WGS84 ellipsoid model of the Earth.

Figure 2 presents the ADS-B data for N2069B near the accident site, plotted in terms of nautical miles north and east of the accident site, and at two different scales. If the position (latitude, longitude, and altitude) of an airplane is known as a function of time, then its orientation (that is, its Euler angles) can also be estimated as long as the following are true:

- The motion of the air mass relative to the Earth, i.e., the wind, is known;
- The lift coefficient (C_L) of the airplane as a function of angle of attack (α) is known;
- The gross weight of the airplane is known;

⁹ "The geoid ... is the shape that the ocean surface would take under the influence of the gravity of Earth, including gravitational attraction and Earth's rotation, if other influences such as winds and tides were absent." (Wikipedia.org, accessed 10/10/2022.)

¹⁰ Per <https://geographiclib.sourceforge.io/cgi-bin/GeoidEval>, the geoid at the accident site is about 21.95 m (72 ft.) below the surface of the WGS84 ellipsoid.

- The sideslip angle and lateral acceleration are negligible (corresponding to coordinated flight).

In this *Study*, the winds aloft are based on a High Resolution – Rapid Refresh (HRRR) model sounding for 10:00 PST over the accident site, obtained from a National Oceanographic and Atmospheric Administration (NOAA) website.¹¹ The wind speed, wind direction, and air temperature as a function of altitude from this model are plotted in Figure 16 (the additional winds plotted in Figure 16 are described below). An altimeter setting of 30.50 “Hg is assumed, which is consistent with the pressure profile in the HRRR sounding and the 10:53 PST Paine Field (KPAE) weather observation.

The 208B lift curve (C_L vs. α) was obtained from the aerodynamic model of the 208B simulation described in section D.6. A gross weight of 7,965 lb. is assumed, corresponding to the predicted weight for condition 5.80L in Raisbeck’s test card for flight 69B-008.

The position coordinates of an airplane as a function of time define its velocity and acceleration components. In coordinated flight, these components lie almost entirely in the plane defined by the airplane’s longitudinal and vertical axes. Furthermore, any change in the *direction* of the velocity vector is produced by a change in the lift vector, either by increasing the magnitude of the lift (as in a pull-up), or by changing the direction of the lift (as in a banked turn). The lift vector also acts entirely in the aircraft’s longitudinal-vertical plane, and is a function of the angle between the aircraft longitudinal axis and the velocity vector (the angle of attack, α). These facts allow the equations of motion to be simplified to the point that a solution for the airplane orientation can be found given the additional information about wind and the airplane lift curve.

The results of the performance calculations based on the ADS-B and winds aloft data are presented along with the results of a simulation of the final 2.4 minutes of the accident flight in Figures 9-15, and are discussed in the sections that follow.

D.4. Radar data

D.4.1. Description of ARSR and ASR radar data

In general, two types of radar are used to provide position and track information, both for aircraft cruising at high altitudes between airport terminal airspaces, and those operating at low altitude and speeds within terminal airspaces.

¹¹ See <https://www.ready.noaa.gov/READYamet.php>.

Air Route Surveillance Radars (ARSRs) are long range (250 nm) radars used to track aircraft cruising between terminal airspaces. ARSR antennas rotate at 5 to 6 RPM, resulting in a radar return every 10 to 12 seconds. Airport Surveillance Radars (ASRs) are short range (60 nm) radars used to provide air traffic control services in terminal areas. ASR antennas rotate at about 13 RPM, resulting in a radar return about every 4.6 seconds. N2069B was tracked by the ASR located near Seattle-Tacoma International Airport (KSEA) (designated "S46"), the ARSR at Fort Lawton in Seattle (designated "SEA"), and the ASR at Naval Air Station (NAS) Whidbey Island (designated "NUW"). The returns corresponding to N2069B from these radar sites are presented in Figure 3 and discussed further below.

D.4.2. Primary and secondary radar returns

A radar detects the position of an object by broadcasting an electronic signal that is reflected by the object and returned to the radar antenna. These reflected signals are called *primary returns*. Knowing the speed of the radar signal and the time interval between when the signal was broadcast and when it was returned, the distance, or range, from the radar antenna to the reflecting object can be determined. Knowing the direction the radar antenna was pointing when the signal was broadcast, the direction (or bearing, or azimuth) from the radar to the object can be determined. Range and azimuth from the radar to the object define the object's position. In general, primary returns are not used to measure the altitude of sensed objects, though some ARSRs do have height estimation capability. ASRs do not have height estimation capabilities.

The strength or quality of the return signal from the object depends on many factors, including the range to the object, the object's size and shape, and atmospheric conditions. In addition, any object in the path of the radar beam can potentially return a signal, and a reflected signal contains no information about the identity of the object that reflected it. These difficulties make distinguishing individual aircraft from each other and other objects (e.g., flocks of birds) based on primary returns alone unreliable and uncertain.

To improve the consistency and reliability of radar returns, aircraft are equipped with transponders that sense beacon interrogator signals broadcast from radar sites, and in turn broadcast a response signal. Thus, even if the radar site is unable to sense a weak reflected signal (primary return), it will sense the response signal broadcast by the transponder and be able to determine the aircraft position. The response signal can also contain additional information, such as the identifying "beacon code" for the

aircraft, and the aircraft's pressure altitude (also called "Mode C" altitude). Transponder signals received by the radar site are called *secondary returns*.

N2069B was flying according to Visual Flight Rules (VFR, as opposed to Instrument Flight Rules, or IFR), broadcasting a "1200" transponder beacon code.

D.4.3. Recorded radar data

Recorded data from the S46 and NUW ASRs and the SEA ARSR was obtained from the FAA, and includes the following parameters:

- UTC time of the radar return, in hours, minutes, and seconds. PST = UTC - 8 hours.
- Transponder beacon code associated with the return (secondary returns only)
- Transponder reported altitude in hundreds of feet associated with the return (secondary returns only). The transponder reports pressure altitude in feet MSL. The resolution of this data is ± 50 ft.
- Slant Range from the radar antenna to the return, in nm. The accuracy of this data is $\pm 1/16$ nm or about ± 380 ft.
- Azimuth relative to magnetic north from the radar antenna to the return, reported in Azimuth Change Pulses (ACPs). ACP values range from 0 to 4096, where 0 = 0° magnetic and 4096 = 360° magnetic. Thus, the azimuth to the target in degrees would be:
(Azimuth in degrees) = $(360/4096) \times$ (Azimuth in ACPs) = $(0.08789) \times$ (Azimuth in ACPs)
The accuracy of azimuth data is ± 2 ACP or $\pm 0.176^\circ$.
- Latitude and longitude coordinates of the radar return, to the nearest arc-second.

The latitude and longitude of the radar returns reported in the radar file are computed from the range and azimuth data sensed by the radar, using the known geographic location of each radar antenna (these calculations are performed by the FAA radar processing systems). In this *Study*, the recorded latitude and longitude coordinates are converted to east and north coordinates from the accident site using the WGS84 ellipsoid model of the earth, and presented in Figure 3.

D.5. Pratt & Whitney FAST engine monitoring data

As noted above, N2069B was equipped with a P&W FAST engine monitoring system. The FAST recorder was sent to Pratt & Whitney Canada for download. The data was recovered successfully and provided to the NTSB.

The FAST data file received by the NTSB contains the parameters listed in Table 1:

Parameter Name	Units	Sample rate from G1000	Curve fit tolerance
Inlet Turbine Temperature (ITT)	°C	10 Hz	1° C
Gas generator speed (Ng)	% RPM	10 Hz	0.15 % RPM
Propeller RPM (Np)	RPM	10 Hz	50 RPM
Oil pressure	psi	5 Hz	1 psi
Oil temperature	°C	5 Hz	1° C
Engine torque	ft.-lb.	5 Hz	10 ft.-lb.
Fuel flow	lb./hr.	5 Hz	5 lb./hr.
Fuel temperature	°C	5 Hz	1° C
Indicated airspeed	KIAS	2 Hz	1 KIAS
Outside air temperature	°C	5 Hz	1° C
Pressure altitude	Ft. MSL	2 Hz	10 ft.

Table 1. Parameters included in FAST data file provided by P&W Canada, with recording tolerances. The parameters in Table 1 highlighted with **bold text** are presented in several of the Figures of this *Study*.

The FAST data does not record data at a uniform sample rate, but only records data when the parameter in question changes by a defined threshold or “tolerance.” As explained by P&W Canada¹² in response to an inquiry from the NTSB,

The FAST box receives and analyzes data from the Garmin G1000 software suite at the rate in which it is transmitted. The FAST box then applies a proprietary data reduction using a linear curve fitting algorithm and “only” stores a new value when the data being received is outside the configured tolerance. This means it is expected that the converted data is not at any specific rate but rather the point in time when the reduction algorithm has detected the parameter to be changing more than the tolerance.

The “Curve fit tolerance” column in Table 1 lists the tolerances for triggering the recording of a new parameter value for each of the FAST parameters.

¹² In an email dated January 11, 2023.

D.6. Simulation of the approach to stall and stall departure

D.6.1. Simulation description and assumptions

A six-degree of freedom simulation of the last two minutes of N2069B's flight (up to the end of the ADS-B data), including the approach to stall and course reversal following the stall break, was performed to generate flight control and throttle inputs that produce a trajectory that is consistent with the ADS-B data, the P&W FAST data, and the capabilities of the airplane. The throttle in the simulation is driven so as to match the engine torque recorded in the FAST data. The simulation outputs can potentially provide additional insight into the circumstances of the accident, though it should be noted that alternative control inputs, which produce similar but slightly different trajectories, could also be generally consistent with the recorded data.

Mathematical simulator models of the 208B aerodynamics, flight control system, and powerplant were provided to the NTSB by KSR and incorporated into the NTSB's own MATLAB-based simulation engine. The KSR models are flight-test validated and qualified to FAA "Level D" full-flight simulator standards.

The temperatures and pressures aloft used in the simulation are those from the 10:00 PST HRRR model sounding. However, the wind speed and direction used in the simulation are different from those in the HRRR sounding, and are instead based on the difference between the true airspeed computed from the indicated airspeed recorded on the FAST and the ground speed recorded in the ADS-B data. The airplane heading is needed for this calculation, and is approximated as the heading computed using the HRRR winds (shown as the "computed heading" in Figure 11). The wind speed and direction computed using the FAST airspeed are shown in Figure 16 as the "computed winds;" for the simulation, these are approximated using the red lines labeled "simulation winds."

The simulation uses a "math pilot" to generate flight control inputs to produce pitch and roll angles that result in an approximate match of the ADS-B position and altitude data, and throttle inputs that match the FAST torque data. The sudden course reversal that occurs at 10:19:05 is likely the result of a large and sudden increase in the roll angle to the left, along with a drop in the pitch angle, associated with the stall break. In the simulation, these motions are approximated using large control inputs (e.g., a large left wheel input to increase the roll angle), rather than by modeling an asymmetric stall. The merit of such an approach is that it confirms that a large roll and reduction in pitch are required to reproduce the trajectory described by the ADS-B data.

While the C_L calculations and the likely test condition (5.80L) at the time of the accident are consistent with the flaps at the LAND setting when N2069B stalled, it is not likely that the flaps were fully deployed throughout the 2.4 minutes preceding the end of the

ADS-B data. Rather, the flaps were likely deployed incrementally as N2069B slowed from 115 KCAS down to just below 50 KCAS at the stall. The exact timing of the flap deployment is unknown, and consequently the flap deployment schedule used in the simulation (and depicted in Figure 13) is an estimate. This estimate has the flaps starting to move from the UP (0°) position at 10:17:20 and reaching the LAND position (26.6°) at 10:17:43.

D.6.2. Simulation results

The results of the simulation are presented in Figures 2 and 8-15. In these Figures, simulation parameters are compared with the corresponding ADS-B or computed parameters, as discussed below.

Figure 2 shows a plan view of the end of the flight. The simulation matches the ADS-B trajectory relatively well, though the course reversal at 10:19:05 is not as “tight” as that depicted by the ADS-B data. This suggests that the left roll following the stall in the actual airplane was faster than that achieved in the simulation using the flight controls, which is not surprising if the (actual) flow separation on the wings was asymmetric.

The north and east simulation coordinates are compared with the ADS-B coordinates as a function of time in Figure 8.

Figure 9 plots altitude vs. time, comparing the ADS-B data with the simulation results and with the FAST pressure altitude. Note that during the final descent the simulation altitude and the “altitude from integrated ADS-B climb rate” lag the ADS-B GNSS altitude. This suggests that in the post-stall dive, the climb rate (vertical speed) recorded in the ADS-B data lags behind the actual climb rate, and that the simulation pitch angle should be a little lower than what the math pilot was able to achieve.

The FAST pressure altitude data in Figure 9c shows a change in slope (vertical speed) following the end of the ADS-B data at about 10:19:18, and a relatively constant rate of descent between that time and impact with the ground. This likely corresponds to the period after the in-flight structural failure of the airplane, and the spiraling descent depicted in Figure 1.

Figure 10 shows the ground speed, true airspeed, calibrated airspeed, and rate of climb computed from the ADS-B and winds aloft data, and output from the simulation. The recorded FAST indicated airspeed during the last minute is also presented, together with the true airspeed computed from the FAST indicated airspeed (up to the end of the ADS-B data). At the time the ADS-B data ends, the calibrated airspeed computed from the ADS-B data and the HRRR winds approximately matches the FAST indicated airspeed at about 200 KCAS. The FAST airspeed jumps to 223 KIAS in the next sample after the end of the ADS-B data, before dropping precipitously. This

suggests that the structural failure occurred around the time of the end of the ADS-B data, and that the sudden jump in the FAST airspeed to 223 KIAS might be an artifact of disrupted flow over the airplane's static ports and / or pitot tube following the failure.

The sudden deceleration shown in the FAST data starting at 10:19:21 is also consistent with the structural failure occurring near this time.

The simulation airspeed does not reach the 200 KCAS computed from the ADS-B and HRRR winds and reflected in the FAST data; this too is consistent with the simulation pitch angle not being steep enough during the post-stall dive.

Figure 11 presents several longitudinal and lateral / directional flight angles for the last 5.5 minutes of flight. The top plot presents the pitch angle (θ) and flight path angle (γ), the middle plot presents roll angle (ϕ) and sideslip angle (β), and the bottom plot presents true heading (ψ) and ground track. As noted in the plots of altitude (Figure 9) and speed (Figure 10), the simulation pitch and flight path angles in the post-stall dive are not as steep as those computed from the ADS-B data. The computed pitch angle reaches -61° , whereas the simulation pitch angle only reaches -53° . This difference is likely the result of the limitations of the math pilot controller and the rapid and relatively extreme dynamics of the maneuver.

The roll angle increases rapidly to the left starting at 10:19:02, as the ailerons are used to force a large left roll angle so as to approximately match the sudden course reversal recorded in the ADS-B data at about 10:19:05 (see Figures 13 and 2). Both the computed and simulation roll angles peak at about -120° , at about the same time that the pitch angle reaches its lowest value.

Figure 12 presents the body-axis load factors during the last 5.5 minutes of flight. The load factors are not remarkable, and neither the computed nor the simulation vertical load factors exceed 2 G's. This finding underscores the fact that when the airspeed limitations of the airplane are exceeded, structural damage can occur even if the load factor limitations are not exceeded.

The simulation flight control inputs and associated flight control surface deflections and control forces are plotted in Figure 13. During the flap transition period between 10:17:20 and 10:17:43, the pitch trim is adjusted to maintain approximately zero column force.

The pitch trim is not adjusted thereafter; approximately 20 lb. of column force is required during the approach to stall, and following the stall the simulation uses up to 40 lb. of column force as the ailerons are used to roll the airplane rapidly to the left. Since the actual roll was likely the result of asymmetries in the flow separation on the wings during the stall, both the pitch and roll control simulation inputs during this time

are not very meaningful. Their purpose is to simply reproduce airplane attitudes that approximately match the trajectory recorded by the ADS-B data.

As noted in Figure 13, the lateral and directional flight control system models are not implemented in this simulation; instead, the control surfaces (ailerons and rudder) are driven directly by the math pilot. However, the pitch control system model is modeled, which is why the simulation column and column force parameters are available, in addition to the elevator parameter.

Figure 14 presents the engine torque recorded in the FAST data (which is used by the math pilot to drive the simulation throttle) and the resulting thrust coefficient (C_T) and horsepower computed by the simulation. The horsepower delivered to the airframe (the required engine thrust multiplied by the true airspeed) computed from the ADS-B data at full flaps is depicted by the dashed black line in Figure 14. The corresponding simulation parameter (simulation thrust multiplied by simulation true airspeed) is depicted by the red line, and the engine shaft horsepower computed by the simulation, corresponding to the engine torque that matches the FAST data, is depicted by the blue line.

Note in Figure 14 that after the stall the FAST torque data does not decrease, but increases from about 907 ft.-lb. at 10:18:51 to 1,075 ft.-lb. at 10:19:09 (just after the pitch and roll angles reach their most extreme values), and then increases dramatically from 1,122 ft.-lb. at 10:19:15 to 1,970 ft.-lb. at the end of the ADS-B data at 10:19:18. The FAST torque peaks at 2,230 ft.-lb. at 10:19:20 before dropping suddenly to 1,033 ft.-lb. at 10:19:22.7 (the last recorded data point).

Figure 15 plots the speed, normal load factor, and lift coefficient (C_L) during the last 2.5 minutes of flight (the airspeed and load factor dictate the C_L that is required). Various values of C_{Lmax} (the maximum C_L that can be produced by the wing, achieved just before the stall) corresponding to different flap settings and data sources are also shown. The red lines correspond to the C_{Lmax} computed from the published stall speeds in the 208B POH (Reference 1). The blue lines correspond to the basic wing landing flaps C_{Lmax} in the KSR 208B aerodynamic model. The simulation C_{Lmax} value varies a little based on engine power, but lies below the both the flaps 20° and landing flaps C_{Lmax} values computed from the POH stall speeds. The reasons for this difference in C_{Lmax} between the simulation aerodynamic model and the POH are unknown.

The black dashed line in Figure 15 is the C_L computed from the ADS-B and winds aloft data. This calculation appears to match the POH landing flaps C_{Lmax} relatively well, and is evidence that the flaps were likely fully deployed at the time of the stall.

D.7. Stall characteristics testing and upset recovery guidance

D.7.1. Upset recovery guidance in the FAA *Airplane Flying Handbook*

The ADS-B and simulation data presented above describe an abrupt roll to the left to about -120° and a drop in pitch to about -60° following a planned partial-power, full-flaps, accelerated stall. During the stall recovery, the airplane accelerated to at least 200 KCAS, which is 75 KCAS above V_{FE} and 25 KCAS above V_{MO} , before a structural failure occurred. Notably, the FAST data indicates that following the stall, the engine torque did not decrease but actually increased, which likely contributed to the airplane's post-stall acceleration.

Chapter 5 of FAA document FAA-H-8083-3C, *Airplane Flying Handbook* (Handbook, Reference 4), titled *Maintaining Aircraft Control: Upset Prevention and Recovery*, references the *Airplane Upset Recovery Training Aid* (Reference 5) in defining an "airplane upset:"

The term "upset" was formally introduced by an industry work group in 2004 in the "Pilot Guide to Airplane Upset Recovery," which is a part of the "Airplane Upset Recovery Training Aid." The work group was primarily focused on large transport airplanes and sought to come up with one term to describe an "unusual attitude" or "loss of control," for example, and to generally describe specific parameters as part of its definition. Consistent with the Guide, the FAA considers an upset to be an event that unintentionally exceeds the parameters normally experienced in flight or training. These parameters are:

1. Pitch attitude greater than 25° , nose up
2. Pitch attitude greater than 10° , nose down
3. Bank angle greater than 45°
4. Within the above parameters, but **flying at airspeeds inappropriate for the conditions**

The reference to inappropriate airspeeds describes a number of undesired aircraft states, including stalls. [emphasis added]

The *Handbook* states that "the pilot should follow the procedures recommended in the AFM/POH" to recover from an upset, and that, "in general, upset recovery procedures are summarized" as follows:

1. Disconnect the wing leveler or autopilot
2. Apply forward column or stick pressure to unload the airplane
3. Aggressively roll the wings to the nearest horizon
4. **Adjust power as necessary by monitoring airspeed** [emphasis added]
5. Return to level flight

The *Handbook* cites the following "common errors associated with upset recoveries:"

1. Incorrect assessment of what kind of upset the airplane is in
2. Failure to disconnect the wing leveler or autopilot

3. Failure to unload the airplane, if necessary
4. Failure to roll in the correct direction
5. **Inappropriate management of the airspeed during the recovery** [emphasis added]

The “stall recovery template” provided in the *Handbook* follows the procedures specified for upsets in general:

1. Wing leveler or autopilot: disconnect
2. a) Pitch nose-down: apply until impending stall indications are eliminated
b) Trim nose-down pitch: as needed
3. Bank: wings level
4. **Thrust/Power: as needed** [emphasis added]
5. Speed brakes/spoilers: retract
6. Return to the desired flight path

The post-stall behavior of N2069B on the accident flight fits the definition of an airplane “upset” provided in the *Handbook*. Since the accident upset followed an accelerated, flaps-down stall, the discussion of this kind of maneuver and its risks in the *Handbook* is of particular interest.

The “Accelerated Stalls” section of the *Handbook* describes these stalls as follows:

At the same gross weight, airplane configuration, CG location, power setting, and environmental conditions, a given airplane consistently stalls at the same indicated airspeed provided the airplane is at +1G (i.e., steady-state unaccelerated flight). However, the airplane can also stall at a higher indicated airspeed when the airplane is subject to an acceleration greater than +1G, such as when turning, pulling up, or other abrupt changes in flightpath. Stalls encountered any time the G-load exceeds +1G are called “accelerated maneuver stalls.” The accelerated stall would most frequently occur inadvertently during improperly executed turns, stall and spin recoveries, pullouts from steep dives, or when overshooting a base to final turn. An accelerated stall is typically demonstrated during steep turns.

A pilot should never practice accelerated stalls with wing flaps in the extended position due to the lower design G-load limitations in that configuration. Accelerated stalls should be performed with a bank of approximately 45°, and in no case at a speed greater than the airplane manufacturer’s recommended airspeed, or the specified design maneuvering speed (V_A) or operating maneuvering speed (V_O). [Emphasis added]

Note that the *Handbook* defines an “accelerated” stall as one which is “encountered any time the G-load exceeds +1G.” The definition of an “accelerated” stall in the test card shown in Figure 7 appears to be different, since conditions 5.8L and 5.80L are both turning stalls (for which the load factor would be greater than 1G), but only condition 5.80L is labeled as “accelerated.” In the test card, “accelerated” refers to the target deceleration for the approach to stall: -1 kt/sec. for condition 5.8L, vs. -3 to -5 kt./sec. for condition 5.80L. This definition is consistent with the language of the regulations discussed in section D.7.2. Of note, condition 5.8L, the first item on the test card for Flight 008, was apparently performed successfully.

The admonition in the *Handbook* against practicing accelerated stalls with the flaps extended suggests an elevated risk to the airplane in this configuration.

The *Handbook* goes on to state:

An airplane typically stalls during a level, coordinated turn similar to the way it does in wings-level flight, except that the stall buffet can be sharper. If the turn is coordinated at the time of the stall, the airplane's nose pitches away from the pilot just as it does in a wings-level stall since both wings will tend to stall nearly simultaneously. If the airplane is not properly coordinated at the time of stall, **the stall behavior may include a change in bank angle** until the AOA has been reduced. It is important to take recovery action at the first indication of a stall (if impending stall training/checking) or immediately after the stall has fully developed (if full stall training/checking) by applying forward elevator pressure as required to reduce the AOA and to eliminate the stall warning, level the wings using ailerons, coordinate with rudder, and **adjust power as necessary**. Stalls that result from abrupt maneuvers tend to be more aggressive than unaccelerated +1G stalls. Because they occur at higher-than-normal airspeeds or may occur at lower-than-anticipated pitch attitudes, they can surprise an inexperienced [pilot, since] **an accelerated stall may put the airplane in an unexpected attitude**. Failure to execute an immediate recovery may result in a spin or other departure from controlled flight. [Emphasis added]

The *Handbook* also contains a section describing "cross-control stalls," which are of interest because of the extreme roll angles that can result. As stated in the *Handbook*,

The aerodynamic effects of the uncoordinated, cross-control stall can surprise the unwary pilot because this stall can occur with very little warning and can be deadly if it occurs close to the ground. The **nose may pitch down, the bank angle may suddenly change, and the airplane may continue to roll to an inverted orientation**, which is usually the beginning of a spin. It is therefore essential for the pilot to follow the stall recovery procedure by reducing the AOA until the stall warning has been eliminated, then roll wings level using ailerons, and coordinate with rudder inputs before the airplane enters a spiral or spin.

...

Before performing this stall, the pilot should establish a safe altitude for entry and recovery in the event of a spin, and clear the area of other traffic while slowly retarding the throttle. The next step is to lower the landing gear (if equipped with retractable gear), **close the throttle**, and maintain altitude until the airspeed approaches the normal glide speed. **To avoid the possibility of exceeding the airplane's limitations, the pilot should not extend the flaps.** [Emphasis added]

The guidance to close the throttle and keep the flaps up while performing a cross-control stall indicates that the risk associated with the maneuver might be increased with power on the airplane and the flaps extended, as they were during the accident. A cross-control stall introduces a sideslip angle at the stall break, which is what can drive asymmetry in the stall and lead to extreme roll angles. Note that the sideslip angle at the time of the accident stall is unknown. However, video of the conduct of condition 5.6L on the previous day's flight in N2069B (Flight 07 Run 16), an "unaccelerated" flaps 30° stall in a left -30° roll with idle thrust, shows the Slip / Skid Indicator bar on the

Primary Flight Display (PFD) displaced about one bar width¹³ to the right just before the airplane stalled (see Figure 17a). According to recorded data for Flight 07, this displacement corresponded to a lateral load factor of about -0.07 G's. In addition, the PFD in Figure 17a depicts a roll angle noticeably greater than the -30° specified for the stall maneuver. After the stall break, the airplane rolled further to the left to a recorded roll angle of -83° and the pitch angle decreased to -45° (see Figure 17b).¹⁴ The engine power was at idle during the maneuver (165 ft.-lb. of torque at the stall break), the deceleration target for the approach to stall was 1 kt./sec., and during the stall recovery the airspeed remained below V_{FE} .

D.7.2. FAA stall characteristics certification standards and flight test guidance

The *Flight Test Plan For Raisbeck Engineering Inc. Drag Reduction System On Textron Aviation Inc. 208B Series Aircraft Model 208B with PT6A-140 Engine (867 SHP) (S/Ns 208B2197 and 208B5000 and on)* (the *Test Plan*), prepared by Aerospace Design & Compliance LLC (AD&C), describes the purpose of the *Test Plan* as follows:

This document provides the step-by-step procedures to verify proper operation of the installation of the Raisbeck Engineering Inc. (REI) Drag Reduction System (DRS) on Textron Aviation Inc. (TAI) Cessna Model 208B Grand Caravan EX model (referred to from herein as "208B EX") aircraft for initial supplemental type certification. These test procedures meet or exceed the requirements to show compliance to the following 14 CFR Part 23 regulations paragraphs:

[List of ten 14 CFR Part 23 regulations]

The list of Part 23 regulations cited in the *Test Plan* includes §23.203 (at Amendment 23-62), *Turning flight and accelerated stalls*. This regulation is cited in the *Test Plan* as follows:

Sec. 23.203 [Turning flight and accelerated turning stalls.] [23-62]

Turning flight and accelerated turning stalls must be demonstrated in tests as follows:

- (a) Establish and maintain a coordinated turn in a 30° bank. Reduce speed by steadily and progressively tightening the turn with the elevator until the airplane is stalled, as defined in §23.201(b). The rate of speed reduction must be constant, and--
 - (1) For a turning flight stall, may not exceed one knot per second; and
 - (2) For an accelerated turning stall, be 3 to 5 knots per second with steadily increasing normal acceleration.

¹³ According to the Garmin G1000 Integrated Flight Deck Pilot's Guide (Reference 6), "one bar displacement is equal to one ball displacement on a traditional inclinometer."

¹⁴ The recorded data does not include pitch angle, so the pitch attitude noted here is based on the video recording of the PFD.

- (b) After the airplane has stalled, as defined in §23.201(b), it must be possible to regain wings level flight by normal use of the flight controls, but without increasing power and without—
- (1) Excessive loss of altitude;
 - (2) Undue pitchup;
 - (3) Uncontrollable tendency to spin;
 - (4) Exceeding a bank angle of 60 degrees in the original direction of the turn or 30 degrees in the opposite direction in the case of turning flight stalls;
 - (5) Exceeding a bank angle of 90 degrees in the original direction of the turn or 60 degrees in the opposite direction in the case of accelerated turning stalls;
and
 - (6) Exceeding the maximum permissible speed or allowable limit load factor.
- (c) Compliance with the requirements of this section must be shown under the following conditions:
- (1) Wings flaps: Retracted, fully extended, and each intermediate normal operating position as appropriate for the phase of flight.
 - (2) Landing gear: Retracted and extended as appropriate for the altitude.
 - (3) Cowl flaps: Appropriate to configuration.
 - (4) Spoilers/speedbrakes: Retracted and extended unless they have no measurable effect at low speeds.
 - (5) Power:
 - (i) Power/Thrust off; and
 - (ii) For reciprocating engine powered airplanes: 75 percent of maximum continuous power. However, if the power-to-weight ratio at 75 percent of maximum continuous power results in nose-high attitudes exceeding 30 degrees, the test may be carried out with the power required for level flight in the landing configuration at maximum landing weight and a speed of $1.4 V_{SO}$, except that the power may not be less than 50 percent of maximum continuous power; or
 - (iii) For turbine engine powered airplanes: The maximum engine thrust, except that it need not exceed the thrust necessary to maintain level flight at $1.5 V_{S1}$ (where V_{S1} corresponds to the stalling speed with flaps in the approach position, the landing gear retracted, and maximum landing weight).
 - (6) Trim: The airplane trimmed at $1.5 V_{S1}$.
 - (7) Propeller: Full increase rpm position for the power off condition.

The wings-level stall is defined in §23.201(b) as follows:

The wings level stall characteristics must be demonstrated in flight as follows. Starting from a speed at least 10 knots above the stall speed, the elevator control must be pulled back so that the rate of speed reduction will not exceed one knot per second until a stall is produced, as shown by either:

- (1) An uncontrollable downward pitching motion of the airplane;
- (2) A downward pitching motion of the airplane that results from the activation of a stall avoidance device (for example, stick pusher); or
- (3) The control reaching the stop.

The *Test Plan* also specifies the procedures to be used when performing the stalls:

PROCEDURE

Turning and Accelerated Stalls [23.203; 23.207]:

1. With the engine at specified power setting, trim the airplane for flight at the target trim speed ($1.5V_s$).
2. Call out trim point.
3. Establish a 30° banked turn.
4. Using elevator only (column), steadily decelerate the airplane into the stall with entry rate no greater than -1.0 knot/second.
5. Call out: initial buffet, stall warning, aft stop, minimum speed.
6. Recover after the aft elevator stop is reached for approximately 2 seconds.
 - a. For Turning stalls: Roll occurring during recovery may not exceed 60° of bank in the original direction of the turn or 30° in opposite direction.
 - b. For Accelerated stalls: Roll occurring during recovery may not exceed 90° of bank in the original direction of the turn or 30° in opposite direction.
7. Allow airplane to stabilize between stalls.
8. Evaluate and comment on airplane handling characteristics.

The procedure above does not specify a deceleration rate of -3 to -5 kt./sec. for accelerated turning stalls (as called for in §23.203(a)(2)), but just after describing these procedures the *Test Plan* presents a table that specifies the “test conditions” at which the stalls are to be performed, and these conditions include the “target entry rate” for the stalls. As reflected in the “remarks” column of the test card shown in Figure 7, the target entry rate for the accelerated turning stalls is indeed -3 to -5 kt./sec. In addition, the “test conditions” listed in the *Test Plan* include both idle power and “power on” conditions. The “power on” condition listed in the test cards (see Figure 7) specifies a torque of 930 ft.-lb., which per the *Test Plan* corresponds to the power required to trim in level flight at $1.5 V_s$ with the flaps in the TO/APR position.

The “test conditions” table in the *Test Plan* also includes a column labeled “Pass/Fail,” which provides a space to record whether the specified stall satisfied the required characteristics specified in §23.203 and in item 6 of the “Procedures” cited above. As noted in section D.7.1 of this *Study*, test condition 5.6L on Flight 07 resulted in a maximum recorded roll angle of -83° , and the post-stall roll angle from this condition depicted on the PFD (see Figure 17b) showed a left roll angle steeper than -60° . Consequently, per the criteria specified in §23.203 and in the *Test Plan* procedures, condition 5.6L should have been considered a “fail,” since the stall was unaccelerated but the resulting roll angle exceeded 60° in the original direction of the turn.

The video from Flight 07 records the crew discussing whether condition 5.6L was a “pass” or “fail.” Table 2 presents relevant portions of this conversation, which took place following a minute-long discussion about how to interpret the column position display presented to the pilot. The peak roll angle of -83° recorded in the flight test data occurred at 15:14:52.

According to Quicksilver Aero (the company contracted to provide instrumentation support for Raisbeck’s flight test program), “engineers in the back [of the airplane] could have had access to the roll angle, and it would have been the same as the -83° [in the recorded data for the flight].”¹⁵

Time	Speaker	Content
15:16:21	Engineer	And were we more than sixty on that roll-off?
15:16:24	Pilot	Uh ... more than sixty ... ah let me think ...
15:16:35	Pilot	No. We were probably about fifty.
15:16:37	Engineer	'K.
15:16:40	Pilot	So technically I guess that's good.
15:16:42	Engineer	It's a pass.
15:16:42	Pilot	That's a pass.
15:16:45	Pilot	So we're going back up to try one to the right.
15:16:46	Engineer	Correct.
15:16:50	Pilot	Glad you mentioned it I was getting ready to reject it.
15:16:54	Pilot	Just 'cause it, it rolled and I couldn't stop it, but ... you know, pushed out ... it was ... it was still within.

Table 2. Crew conversation concerning the magnitude of roll angle achieved during condition 5.6L on Flight 07, as transcribed from the video recording of the flight.

FAA Advisory Circular (AC) 23-8C, *Flight Test Guide for Certification of Part 23 Airplanes*, describes its purpose follows:

This advisory circular (AC) sets forth an acceptable means, but not the only means, of showing compliance with Title 14 of the Code of Federal Regulations (14 CFR) part 23 concerning flight tests and pilot judgements. Material in this AC is neither mandatory nor regulatory in nature and does not constitute a regulation.

...

This material is intended as a ready reference for part 23 airplane manufacturers, modifiers, Federal Aviation Administration (FAA) design evaluation engineers, flight test engineers, and engineering flight test pilots, including Organization Delegation Option (DOA).

Section 7.2 of AC 23-8C discusses 14 CFR §23.203 (turning flight and accelerated turning stalls), and lists procedures for demonstrating compliance with this regulation. These procedures include “test pilot determinations,” among which are that the “roll does not exceed the value specified in the requirements” and that “for accelerated turning stalls, maximum speed or limit load factors [are] not exceeded.”

D.7.3. Risk mitigation in the Test Plan and the Flight Test Safety Database

Flight testing of new airplane designs involves inherent risks, because it is not known whether those designs satisfy the relevant certification requirements (the purpose of the testing is to find out). The DRS flight-test campaign described by AD&C’s *Test Plan*

¹⁵ Per an email from Quicksilver Aero to the author, dated 01/12/2024.

involved testing the baseline 208B EX's stall characteristics, and so the risks associated with such testing (as described in section D.7.1) were present during that campaign. However, the 208B EX modified with the APE III STC is (and was at the time) a certified airplane, and so had already demonstrated compliance with the regulations cited in the *Test Plan*. Consequently, it could be argued that the risk involved in stall-testing N2069B was lower than that associated with testing a new and unknown design. Nonetheless, the content of the *Test Plan* reflects an intent to approach the DRS testing with the same conservatism and risk-mitigation that would be expected when testing a new design; the *Test Plan* itself states that "an assessment of the hazards associated with the test program defined in this flight test plan was conducted using the guidelines contained in FAA Order 4040.26C." FAA Order 4040.26C, *Aircraft Certification Service Flight Test Risk Management*, states that:

This order establishes flight test risk management program requirements for the Federal Aviation Administration (FAA) Aircraft Certification Service (AIR). Anyone participating in certification flight test activities must observe all elements of this order

Appendix A of the *Test Plan* contains Test Hazard Analysis (THA) Worksheets for each of the "test types" identified in the *Test Plan*. Each THA can be identified by the "Hazard Number" it addresses; the THA for Hazard Number 9.5 (THA 9.5), addressing Aft CG Stall Characteristics, is duplicated here as Figure 18.

As shown in Figure 18, THAs identify the test type, the hazards associated with the test, the "cause" and "effect" of the hazard, and "mitigations and minimizing procedures" to avoid the hazard. In addition, "emergency procedures" are identified to recover the airplane in case the hazard is in fact encountered (for example, in case the airplane departs from controlled flight). The THA is assigned an overall "risk assessment" (low, medium, or high) depending on the combination of the severity of the effects of the hazard and the probability of the hazard being encountered.

For THA 9.5, the identified hazard is "departure from controlled flight." The "causes" of the hazard are "unpredicted aerodynamic response" and "improper control inputs," and the "effect" of the hazard is "loss of significant amount of altitude which leads to a ground impact." An increase in airspeed and aerodynamic loads above the airplane's limitations are not identified as "effects" of the "departure from controlled flight" hazard.

The "emergency procedures" section of THA 9.5 describes the steps for arresting and recovering from an "unintentional spin," and references the POH/AFM Emergency Procedures section. Recovery from an overspeed condition is not mentioned. However, the first step in the spin recovery procedure is to "retard power to idle position," which helps to avoid an excessive increase in airspeed while the airplane is in a nose-low attitude.

The overall risk assessment assigned to THA 9.5 is “medium.”

The “hazard” and “causes” identified in THA 9.5 mirror those identified in the THA for stall characteristics testing (THA 56) contained in the *Flight Test Safety Database* (FTSD)¹⁶ maintained by the National Aeronautics and Space Administration (NASA) and duplicated here as Figure 19. However, THA 56 in the FTSD includes some mitigations not listed in THA 9.5 of the *Test Plan*, including these three that appear particularly relevant to the N2069B accident:

- 1b. Terminate buildup if FAR limits on bank angle are exceeded at any point of the buildup.
- 9. No aggravated input stalls. All stalls will be ball centered.
- 11. If departing controlled flight retard throttles to idle and centralize controls.

In addition, the overall risk assessment assigned to THA 56 is “high.”

The “buildup approach” to stall testing (that is, the testing of lower-risk conditions before proceeding to higher-risk conditions) advocated in THA 56 is mirrored in the order of tests prescribed in the *Test Plan* and depicted in the test card shown in Figure 7. However, mitigation 1b in THA 56 (termination of the buildup if the roll angle limits are exceeded) is not included in the mitigations listed in the *Test Plan*. This omission appears particularly relevant given the roll to -83° during condition 5.6L on Flight 07, and the apparent roll to about -120° following the execution of condition 5.80L during the accident flight. The logic of mitigation 1b suggests that the roll exceedance following condition 5.6L should have been identified, and the possible reasons for it determined (for example, the Slip/Skid indicator not being centered at the stall break, or perhaps an asymmetry in N2069B’s airframe), before the testing proceeded to higher-risk conditions, such as power-on condition 5.80L (which is higher risk compared to the idle-power condition of condition 5.6L).

D.7.4. Stall and overspeed guidance in the 208B POH and Maintenance Manual

Stall guidance in the 208B Pilot’s Operating Handbook is contained in the “Normal Procedures” section, and states:

Stall characteristics are conventional and aural warning is provided by a stall warning horn which sounds between 5 and 10 knots above the stall in all configurations.
Refer to Section 5, Performance, Figure 5-6 [of the POH], for idle-power stall speeds at maximum weight for both forward and aft C.G. limits.

NOTE

Practice of stalls should be done conservatively and with sufficient altitude for a safe recovery.

¹⁶ See <https://ftsdb.grc.nasa.gov/>.

The POH prohibits intentional spins. In the event of an inadvertent spin, the “Emergency Procedures” section of the POH provides the spin recovery steps shown in THA 9.5 of the *Test Plan* (see Figure 18).

The Cessna 208 Series Maintenance Manual (Reference 7) includes a section titled *Unscheduled Maintenance Checks*. This section states that when an overspeed (among other events) is reported by the flight crew,

a visual inspection of the airframe and specific inspections of components and areas involved must be accomplished. The inspections are performed to determine and evaluate the extent of damage in local areas of visible damage, and to structure and components adjacent to the area of damage.

The Maintenance Manual defines an “overspeed” as follows:

- (1) Any time an airplane has exceeded one or both of the following:
 - a. Airplane overspeed exceeding placard speed limits of flaps.
 - b. Airplane overspeed exceeding design speeds.
- (2) Airplanes equipped with an airspeed exceedance device capable of recording an airspeed exceedance with accompanying time duration:
 - a. For a recorded airspeed above 175 knots in smooth air, with duration greater than 5 seconds, or any airspeed above 181 knots, perform the specified overspeed inspection.

The video recording of Flight 07 on the day before the accident indicates that at the end of that day’s testing, following a pitch-over to “recover airspeed” (as stated by the pilot), the airplane exceeded V_{MO} (175 KIAS) for over 6 seconds and reached a peak airspeed of 183 KIAS (see Figure 20). This condition would have satisfied the requirements for the overspeed inspection described in the Maintenance Manual, but the investigation did not find any record of an overspeed inspection. According to the copilot on Flight 07¹⁷, the overspeed condition was not recorded in the airplane’s logbook.

The omission of a record of the overspeed condition and of the required inspection was inconsistent with the guidance in FAA Order 4040.26C. Appendix B of the Order, titled *FAA Flight Test Briefing Guide*, contains “a detailed list of most things that should be covered in a thorough pre- and post-flight briefing.” Among the items listed in the “Post-Flight” section of the Appendix are the following (emphasis added):

11. Discussion of test conduct:
 - Safety Review/Discussion.
 - Review all test cards.
 - Were all test points executed satisfactorily?

¹⁷ Per an email to the NTSB IIC dated 02/07/2024.

- **Were any limits approached or exceeded?**
- **Are any visual or other inspections required? (e.g., due to exceedance).**
- Were the required data gathered?
- Was build-up adequate?
- Was risk level accurate?
- Are any repeats necessary?
- Were there any unusual events?
- What events prompted questions that were never adequately answered?
- Chase/ground observations.

An effective review of these items after Flight 07 might have identified the V_{MO} exceedance as an event requiring an inspection per the Maintenance Manual. Such a review might also have called attention to the excessive roll on condition 5.6L.

D.7.5. Additional upset recovery guidance

As noted above, the FAA *Airplane Flying Handbook* references the *Airplane Upset Recovery Training Aid* (Reference 5) in its discussion of airplane upsets. Section 2.6.3 of the *Training Aid*, titled *Airplane Upset Recovery Techniques*, presents techniques for recovering from various upset scenarios, including stalls and “high bank angles.” The techniques advocated in the *Training Aid* were developed specifically for transport-category airplanes, but the general concepts involved are relevant to all airplane types.

The following situation presented in the *Training Aid* describes the condition of N2069B immediately after the stall that preceded the structural failure of the airplane:

Situation: Bank angle greater than 45 deg.
 Pitch attitude lower than 10 deg, nose low.
 Airspeed increasing.

A nose-low, high-angle-of-bank attitude requires prompt action, because altitude is rapidly being exchanged for airspeed. Even if the airplane is at an altitude where ground impact is not an immediate concern, **airspeed can rapidly increase beyond airplane design limits.** Recognize and confirm the situation. Disengage the autopilot and autothrottle. Simultaneous application of roll and **adjustment of thrust** may be necessary. ... Full aileron and spoiler input may be necessary to smoothly establish a recovery roll rate toward the nearest horizon. ... If the application of full lateral control (ailerons and spoilers) is not satisfactory, it may be necessary to apply rudder in the direction of the desired roll. ... Complete the recovery by establishing a pitch, thrust, and airplane drag device configuration that corresponds to the desired airspeed. ... [Emphasis added]

For smaller, general aviation airplanes, the Airplane Pilots and Owners Association (AOPA) has also published upset recovery guidance. An AOPA online article titled *Technique: Unusual Attitude – Shaking Up Your Inner Ear*¹⁸ includes the graphic

¹⁸ See <https://www.aopa.org/news-and-media/all-news/2017/june/flight-training-magazine/technique-unusual-attitude>.

reproduced here as Figure 21. Note that the graphic states that the first step in the recovery technique from a nose-low attitude is to “bring power to idle.” The second and third steps in the recovery are the leveling of the wings and the raising of the nose, respectively.

The FAA *Airplane Flying Handbook*, the industry *Upset Recovery Training Aid*, the *Flight Test Safety Database* THA 56, and AOPA’s online article all note the importance of reducing power in a nose-low unusual attitude (resulting from an “upset” that can include a stall) in order to avoid airspeed exceedances that can damage the airplane. Of note, the *Handbook* advises pilots to avoid accelerated stalls with wing flaps extended altogether, since the airspeed and load factor limitations of this configuration are more restrictive.

As noted above, following the condition 5.80L stall on the accident flight, the engine torque did not decrease, but increased. This likely contributed to the rapidity with which the airplane accelerated past V_{FE} and V_{MO} . To quantify the difference a reduction in torque would have made on N2069B’s post-stall airspeed behavior, the simulation of the stall maneuver was repeated, keeping the math pilot control logic the same as in the original simulation but forcing the engine power to idle over 4 seconds after the pitch angle decreases below -10° following the stall. The results of this second simulation are compared to the original simulation in Figure 22.

As shown in Figure 22, in the original simulation (which matches the engine torque recorded by the FAST), the final airspeed is about 178 KCAS (though, per Figure 10, the actual airspeed was probably closer to 200 KCAS). In the second simulation (in which the power is reduced to idle after the stall), the final airspeed is about 161 KCAS (a 10% reduction from 178 KCAS). However, the dynamic pressure (which depends on the square of the airspeed) decreases from 106 lb./ft.² in the original simulation to 87 lb./ft.² in the second simulation, a reduction of 18%. The aerodynamic forces on the airplane are proportional to the dynamic pressure, so the second simulation indicates that reducing the power to idle following the stall might have reduced the aerodynamic forces during the period simulated by about 18%.

E. CONCLUSIONS

The material in this *Study* supports a number of observations regarding the performance of N2069B leading up to the structural failure it experienced during the attempted recovery from a planned accelerated, flaps-down, partial power stall, which was conducted as part of a flight-test of the flight characteristics of 208B Grand Caravan EX modified with the APE III STC in support of developing baseline performance for certification of Raisbeck’s DRS system for that airplane. The sequence of events leading up to the stall, attempted recovery, and structural failure are detailed in section C.3.

Analysis of the ADS-B data for the flight, and a simulation that approximately matches the airplane trajectory recorded by the ADS-B data, indicate that following the stall N2069B rolled rapidly to the left, reaching a left roll angle of about -120° , while the pitch angle simultaneously decreased to about -60° . Critically, the airspeed during this time increased rapidly, exceeding both the maximum flaps extended speed with landing flaps (V_{FE}) and the airplane's maximum operating speed (V_{MO}). In addition, the FAST data recorded for the flight indicates that after the stall, the engine torque did not decrease but instead increased, which likely contributed to the rapidity with which the airspeed increased. A second simulation of the stall maneuver indicates that had the engine power been reduced to idle after the nose dropped below -10° pitch following the stall break, the airspeed during the period simulated (up to the end of the ADS-B data) might have been reduced by 10%, corresponding to a reduction in dynamic pressure (and aerodynamic loads) of 18%.

The FAA *Airplane Flying Handbook* identifies the risk of an airplane upset associated with stall maneuvers, and advises pilots to avoid accelerated stalls (where the stall break occurs at a load factor greater than 1-G) with the flaps deployed because the airplane limitations in this configuration are more restrictive and hence more easily exceeded. Both the *Handbook* and the *Airplane Upset Training Aid* note that proper management of engine power / thrust is required during upset recoveries in order to avoid exceeding airspeed limitations. In addition, a graphic AOPA published as a guide to unusual attitude recovery (Figure 21) notes that the first step in recovering from a nose-low attitude is to "bring power to idle."

The 208B EX modified with the APE III STC is a certified airplane, and its compliance with the stall characteristics of §23.203 has already been demonstrated. Consequently, it could be argued that there was less risk in stall testing N2069B than in testing a new, unknown design. Nonetheless, the buildup of the stall tests and the corresponding THAs specified in the *Test Plan* reflect an intent to test using the same risk analyses and mitigations as are used for a new design, and are generally consistent with guidance in FAA AC 23-8C and NASA's FTSD. However, video of the tests conducted during Flight 07, the day before the accident, records a couple of instances of a lack of rigor in the execution of the *Test Plan* and the operation of the airplane. Specifically,

- The test crew failed to identify the exceedance of the roll angle limits during condition 5.6L, which would have rendered that condition a "failed" test.
- The airplane was apparently not inspected after exceeding V_{MO} shortly after the termination of testing on Flight 07, as required by the 208B maintenance manual.

In light of these findings, the omission of the following risk mitigations listed in THA 56 of the FTSD from THA 9.5 of *Test Plan* appear relevant to the accident flight:

- Stop the test buildup if the roll limits are exceeded during a test (this mitigation implies a need to determine the reasons for the exceedance, and to implement corrective actions before proceeding to higher-risk conditions in the test plan).
- Bring the throttle to idle if departing controlled flight (THA 9.5 mentions spins specifically - recovery from which includes retarding the throttle - but "departure from controlled flight" is not limited to spins, and includes unintentional unusual attitudes).

Submitted by:

John O'Callaghan
National Resource Specialist - Aircraft Performance

F. REFERENCES

1. Cessna Aircraft Company, *Grand Caravan EX Pilot's Operating Handbook and FAA Approved Airplane Flight Manual*, Revision 1, 22 May 2013, Part number 208BPHCUS-01.
2. National Transportation Safety Board, *Aviation Investigation Preliminary Report: Cessna 208B, N2069B, Snohomish, WA, November 18, 2022, NTSB Accident Number WPR23FA034*.
3. International Civil Aviation Organization (ICAO), *The Tenth Meeting of Automatic Dependent Surveillance - Broadcast (ADS-B) Study and Implementation Task Force (ADS-B SITF/10) Agenda Item 6: Review States' activities and interregional issues on trials and implementation of ADS-B and multilateralism: ADS-B / GPS Accuracy (Presented by Australia)*. Singapore, 26-29 April 2011. Document available at:
https://www.icao.int/APAC/Meetings/2011_ADS_B_SITF10/IP10_AUS%20AI%206%20-%20GPS%20Accuracy.pdf.
4. Federal Aviation Administration, *Airplane Flying Handbook*, document FAA-H-8083-3C, issued 2021. Available at: https://www.faa.gov/regulations_policies/handbooks_manuals/aviation/airplane_handbook.
5. Upset Recovery Industry Team, *Airplane Upset Recovery Training Aid*, Revision 2, November 2008. Available at: https://www.faa.gov/sites/faa.gov/files/pilots/training/AP_UpsetRecovery_Book.pdf.
6. Garmin, *Cessna Nav III G1000 Integrated Flight Deck Pilot's Guide*, document 190-00498-08 Rev. A, May 2013. Available at: https://static.garmin.com/pumac/190-00498-08_0A_Web.pdf.
7. Cessna Aircraft Company, *Maintenance Manual: 1985 & On Model 208 Series*, Revision 39, 1 March 2023.
8. Textron Aviation, *Air Safety Investigations Aircraft Incident/Accident Technical Report*, Report # ASI-22-CT-T, dated 06-05-23. (Available through the NTSB CAROL search tool at <https://data.nts.gov/carol-main-public/landing-page>).

G. GLOSSARY

Acronyms

AC	Advisory Circular
ADS-B	Automatic Dependent Surveillance - Broadcast
AD&C	Aerospace Design & Compliance LLC
AFM	Airplane Flight Manual
AGL	Above ground level
AOPA	Airplane Owners and Pilots Association
APE III	AeroAcoustics Aircraft Systems Aircraft Payload Extender
ARSR	Air Route Surveillance Radar
ASR	Airport Surveillance Radar
ATC	Air Traffic Control
CFR	Code of Federal Regulations
CG	Center of Gravity
CVR	Cockpit Voice Recorder
DRS	Drag Reduction System
FAA	Federal Aviation Administration
FAST	P&W Full Flight Data Acquisition, Storage, and Transmission engine monitor
FDR	Flight Data Recorder
FTD	Flight Training Device
FTSD	NASA Flight Test Safety Database
GNSS	Global Navigation Satellite System
GPS	Global Positioning System
"Hg	Inches of mercury
HRRR	High Resolution - Rapid Refresh atmospheric model
IIC	NTSB Investigator In Charge
KCAS	Knots calibrated airspeed
KIAS	Knots indicated airspeed
KSEA	Seattle-Tacoma International Airport
KSR	Kohlman Systems Research
KTAS	Knots true airspeed
MSL	Mean Sea Level
NAS	Naval Air Station
NASA	National Aeronautics and Space Administration
NTSB	National Transportation Safety Board
NUW	ASR at NAS Whidbey Island
PFD	Primary Flight Display
POH	Pilot's Operating Handbook
PST	Pacific Standard Time
P&W	Pratt & Whitney
REI	Reisbeck Engineering Incorporated
S46	ASR located near KSEA
SEA	ARSR at Fort Lawton in Seattle, Washington
STC	Supplemental Type Certificate
THA	Test Hazard Analysis
UTC	Universal Coordinated Time

Symbols

α	Angle of attack
β	Sideslip angle
γ	Flight path angle
θ	Pitch angle
ϕ	Roll angle
ψ	Heading angle
C_L, C_{Lmax}	Lift coefficient, maximum lift coefficient
nlf	Normal load factor
n_y	Lateral load factor
V_{FE}	Maximum flaps extended speed with landing flaps
V_{MO}	Maximum operating speed

FIGURES



Figure 1. Photograph of N2069B spiraling to the ground provided by a witness (left), and composite of frames from a security camera video of the same (right). The images on the right show the left wing attached to the fuselage and the right wing missing. (Images taken from the NTSB preliminary report of the accident (Reference 2).)

WPR23FA034: Cessna 208B, N2069B, Snohomish, WA, 11/18/2022

Plan view of flight path over accident area

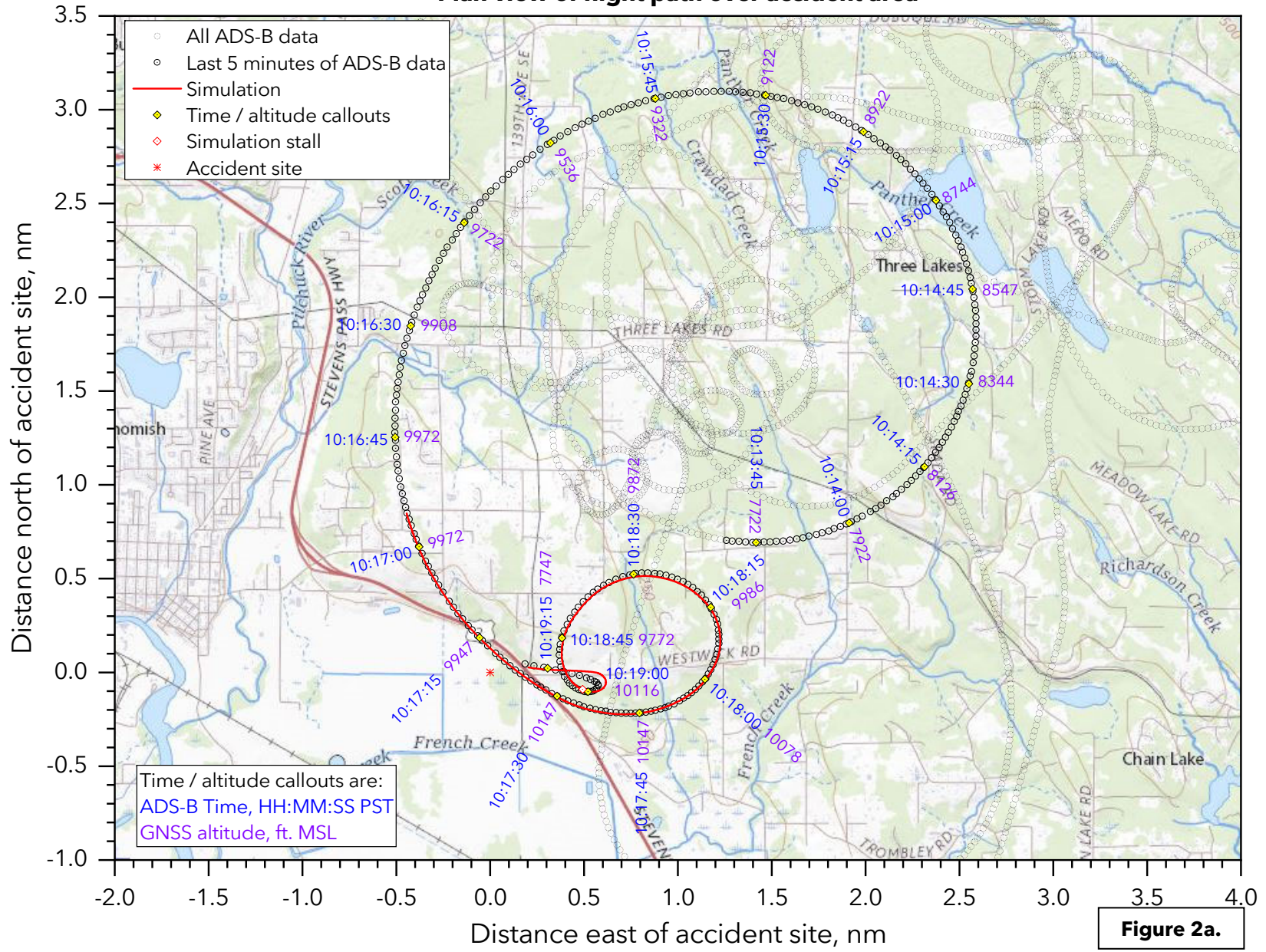
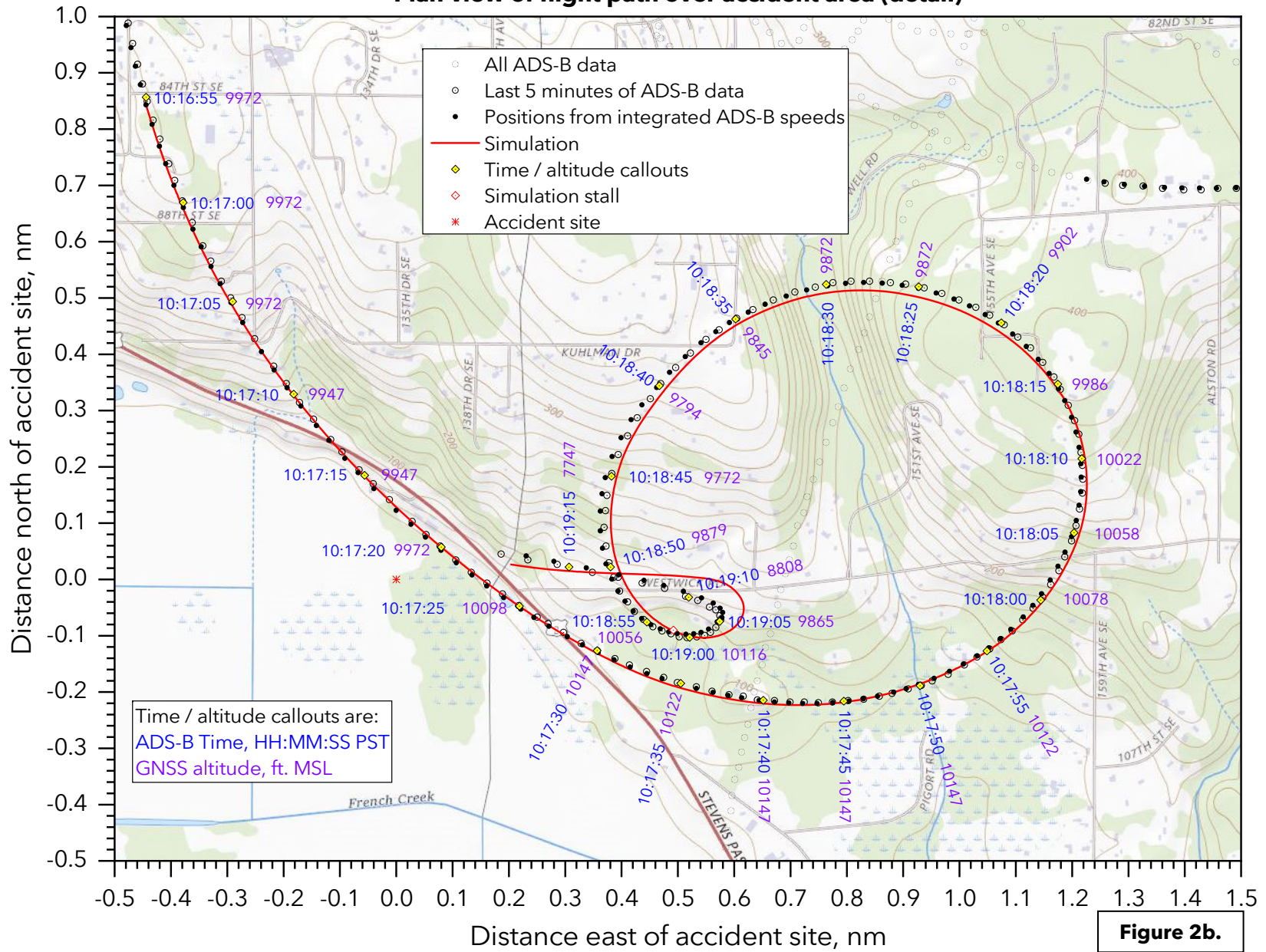


Figure 2a.

WPR23FA034: Cessna 208B, N2069B, Snohomish, WA, 11/18/2022

Plan view of flight path over accident area (detail)



WPR23FA034: Cessna 208B, N2069B, Snohomish, WA, 11/18/2022

Radar tracks with primary returns

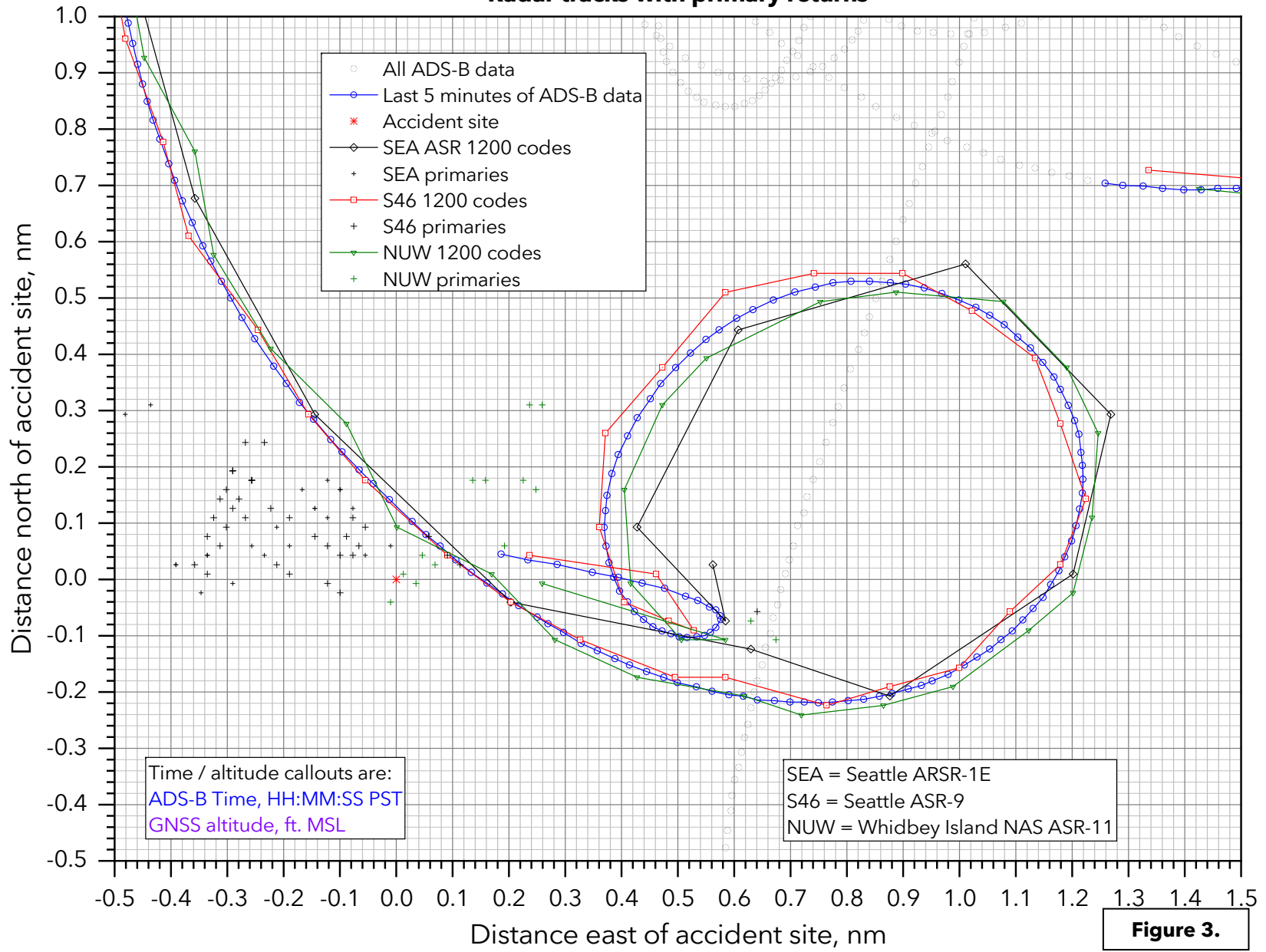


Figure 3.



Figure 4. Pre-accident and pre-APE III STC photograph of N2069B (photo credit: Robert Eikelenboom via aviation-safety.net).

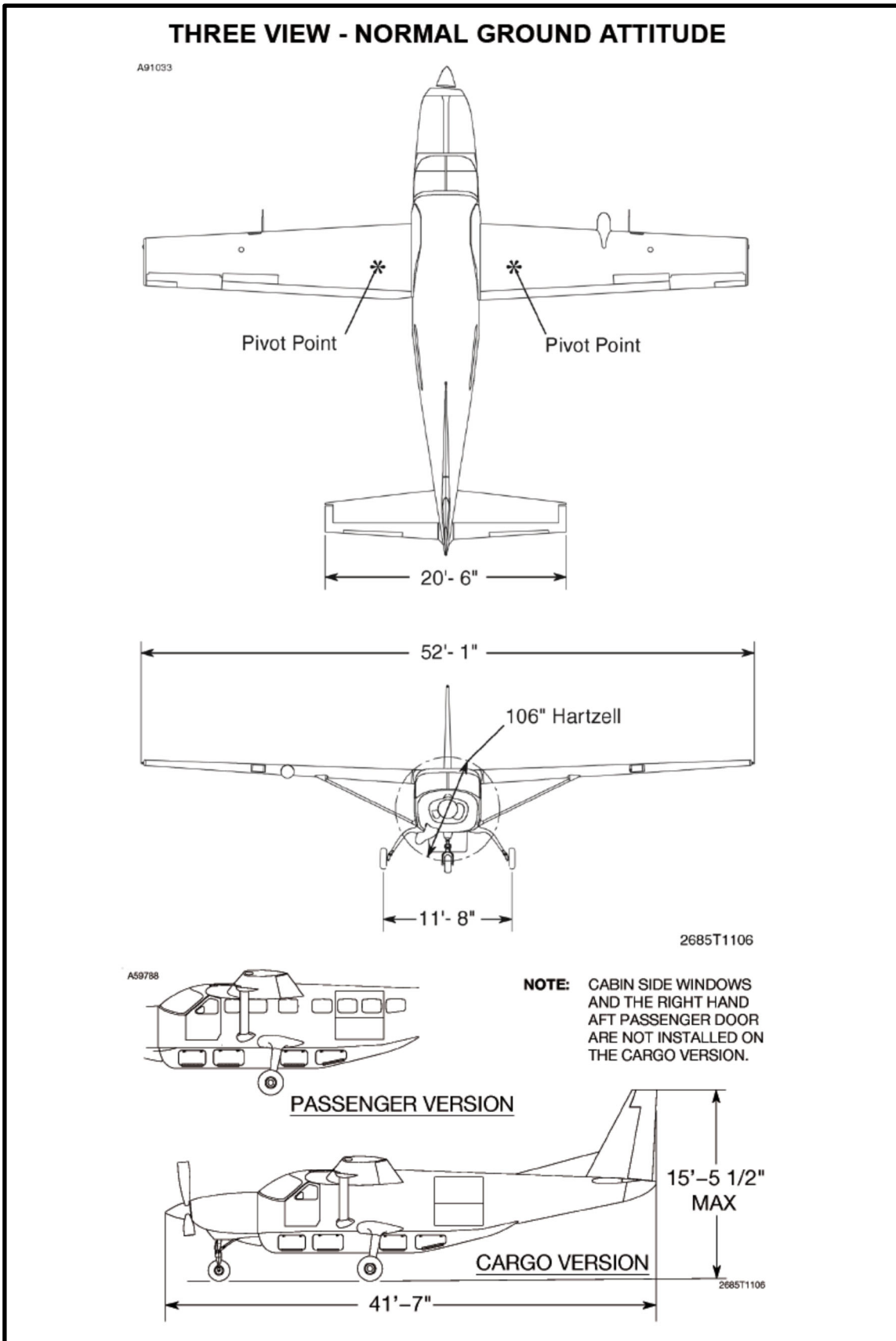


Figure 5. Three-view drawings of the Cessna 208B Grand Caravan EX, from Reference 1.

WEIGHT AND BALANCE ~ AIRCRAFT LOADING

CESSNA 208B EX S/N: 208B5657 R/N: N2069B

FLIGHT No.: 69B-008 DATE: 11/18/2022 REVISION: IR

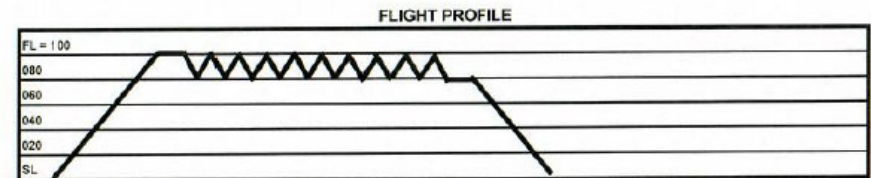
Item Description	Personnel Name	Weight lb	Fus. Sta in	C.G. % Mac	Moment lb-in
<u>Empty Weight (11/15/2022)</u>		5,601.9	191.17	20.48	1,070,897.9
<u>Crew</u>					
	Pilot: [REDACTED]	180.0	139.5		25,110
	Co-Pilot: [REDACTED]	165.0	142.5		23,513
	Test Director/2nd Row Bench Laptop&AFM moved aft	-6.0	179.7		-1,078
	Test Director (Aft CG Position) [REDACTED]	241.0	288.0		69,408
	Instrumentation Lead [REDACTED]	153.0	286.0		43,758
<u>Modifications</u>					
	Foward Fairing and System (31.5 lb) Not installed	0.0	93.16		
	Aft Strakes (5.9 lb) Not installed	0.0	402.98		
<u>Fuselage Cargo Configuration</u>					
	Zone 1 Max Load 1780 lbs		172.10		
	Zone 2 Max Load 3100 lbs		217.80		
	Zone 3 Max Load 1900 lbs		264.40		
	Zone 4 Max Load 1380 lbs		294.00		
	Zone 5 Max Load 1270 lbs	125.0	327.00		40,875
	Zone 6 Max Load 320 lbs	300.0	344.00		103,200
	Total Max Load To Not Exceed 3400 lbs				
<u>Cargo Pod</u>					
	Zone A(Max Weight 230 lbs) Max Floor Load 30 lbs/ft ²		132.40		
	Zone B(Max Weight 310 lbs) Max Floor Load 30 lbs/ft ²		182.10		
	Zone C(Max Weight 270 lbs) Max Floor Load 30 lbs/ft ²		233.40		
	Zone D(Max Weight 280 lbs) Max Floor Load 30 lbs/ft ²		287.60		
<u>Instrumentation:</u>					
	DAS Cabin (included in EW)	0.0	246.0		
ZERO FUEL WT (MAX 8,807 LB):		6,760	203.51	39.06	1,375,683
Fuel, lb(Max useable 335.3 gal, 2,246 lb @ 6.7 lb/gal Wings and Reservoir		1738	203.19		353,146
RAMP WEIGHT (MAX 9,097 LB):		8,498	203.44	38.96	1,728,830

Loading Summary
 Total Occupant Load (LB): 733
 Modification Load (LB): 0
 Total Fuselage Cargo Load (LB): 426
 Total Cargo Pod Load (LB): 0
 Instrumentation Load (LB): 0
 Total Usable Fuel Load (LB): 1738.00
 Ramp C.G. (%MAC): 38.96

Figure 6. Weight-and-balance form for flight 69B-008, prepared by Raisbeck Engineering.

RAISBECK CESSNA 208B EX FLIGHT TEST CARD

Flight: 69B-008 Date: 11/18/2022
 Aircraft Tail Number: N2069B Flight Type: Alt CG Stall Characteristics
 Aircraft Serial Number: 206B5657 Airport: KRNT
 Configuration: Baseline
 ZFW: _____ Fuel: _____ RMP Wt: _____
 Temp: _____ Flaps: _____ TOFL: _____
 V1: _____ VR: _____ V2: n/a
 C.G.: _____ Slab: n/a LND Wt: _____

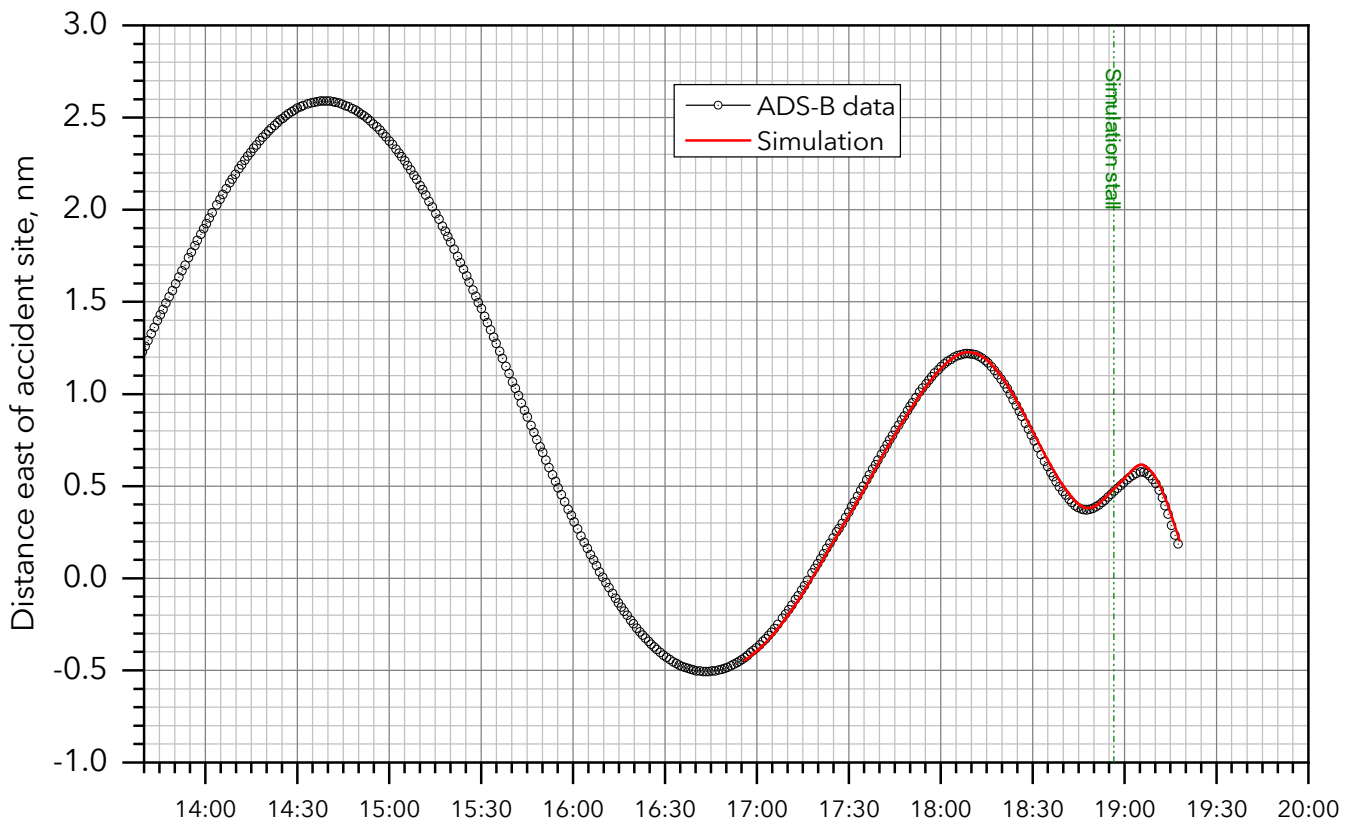
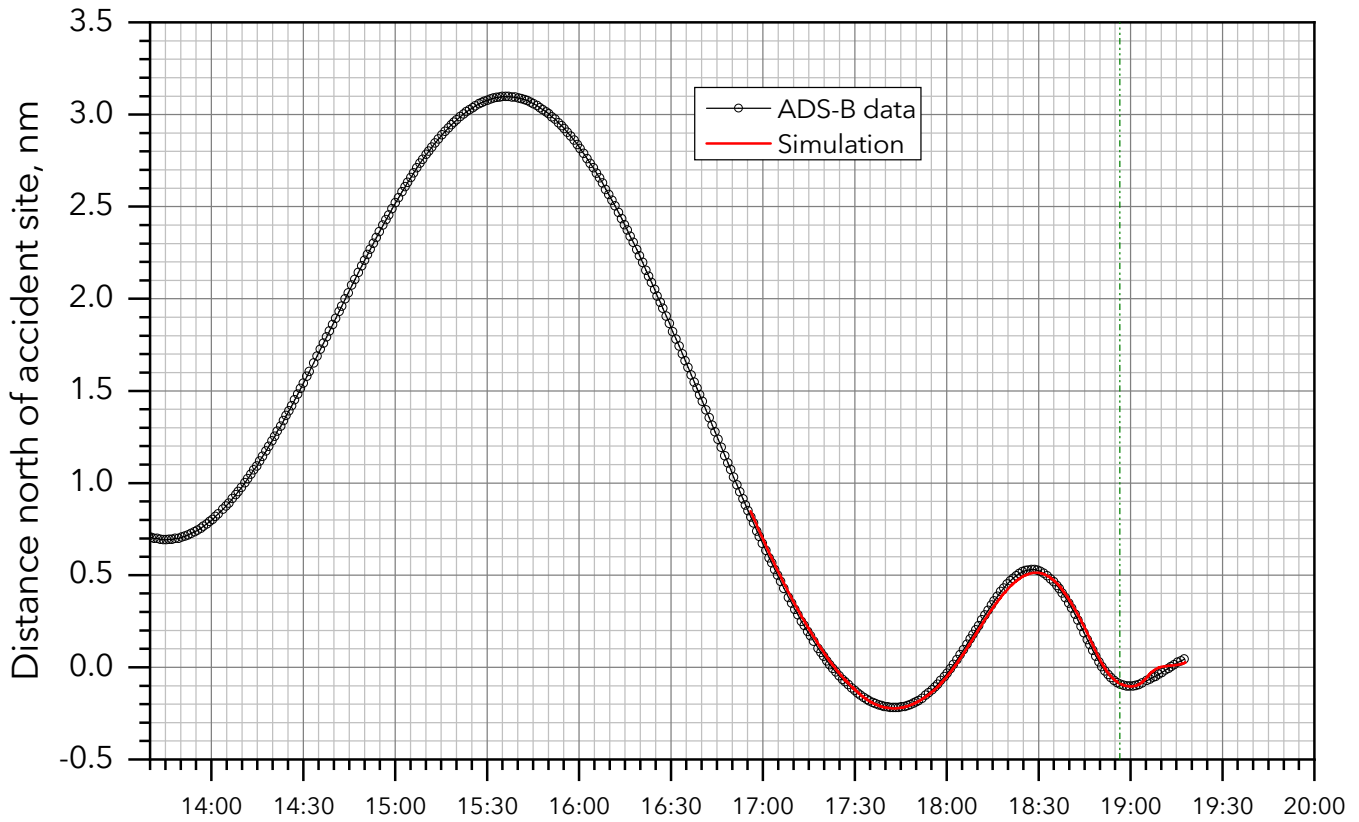


COND	Altitude	Target Speed KIAS	FLAP	Torque Ft-Lb	Propeller RPM	APPROX WEIGHT	FUEL REMAINING	REMARKS
Takeoff	Airport	(83/104)	Up	2397	1900	8,498	1,738	Normal takeoff. Make note of handling characteristics
5.8L	7,000-10,000	1.5 Vs (96)	Land	930	Full Fwd	8,385	1,625	Turning 30° Bank Left. Target -1.0 kt/sec
5.8R	7,000-10,000	1.5 Vs (96)	Land	930	Full Fwd	8,369	1,609	Turning 30° Bank Right. Target -1.0 kt/sec
5.50L	7,000-10,000	1.5 Vs (126)	Up	Idle	Full Fwd	8,304	1,544	Accelerated 30° Bank Left. Target -3.0 kt/sec to -5.0 kt/sec
5.50R	7,000-10,000	1.5 Vs (126)	Up	Idle	Full Fwd	8,239	1,479	Accelerated 30° Bank Right. Target -3.0 kt/sec to -5.0 kt/sec
5.70L	7,000-10,000	1.5 Vs (126)	Up	930	Full Fwd	8,175	1,415	Accelerated 30° Bank Left. Target -3.0 kt/sec to -5.0 kt/sec
5.70R	7,000-10,000	1.5 Vs (126)	Up	930	Full Fwd	8,158	1,398	Accelerated 30° Bank Right. Target -3.0 kt/sec to -5.0 kt/sec
5.60L	7,000-10,000	1.5 Vs (96)	Land	Idle	Full Fwd	8,094	1,334	Accelerated 30° Bank Left. Target -3.0 kt/sec to -5.0 kt/sec
5.60R	7,000-10,000	1.5 Vs (96)	Land	Idle	Full Fwd	8,029	1,269	Accelerated 30° Bank Right. Target -3.0 kt/sec to -5.0 kt/sec
5.80L	7,000-10,000	1.5 Vs (96)	Land	930	Full Fwd	7,965	1,205	Accelerated 30° Bank Left. Target -3.0 kt/sec to -5.0 kt/sec
5.80R	7,000-10,000	1.5 Vs (96)	Land	930	Full Fwd	7,948	1,188	Accelerated 30° Bank Right. Target -3.0 kt/sec to -5.0 kt/sec
Land	Airport	72	Land	As req'd	Full Forward	7,884	1,124	Normal landing. Make note of handling characteristics

Figure 7. Flight test card for flight 69B-008, prepared by Raisbeck Engineering.

WPR23FA034: Cessna 208B, N2069B, Snohomish, WA, 11/18/2022

North & east coordinates vs. time



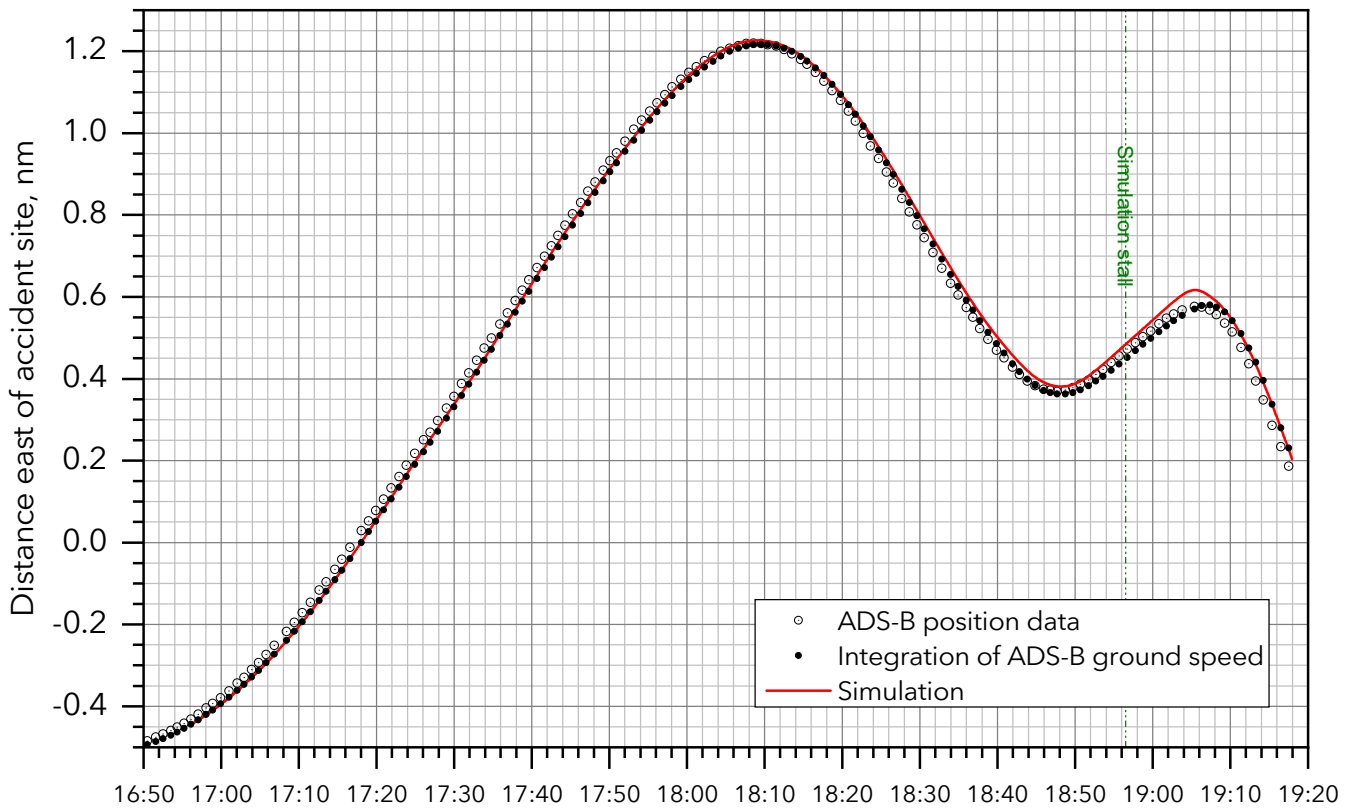
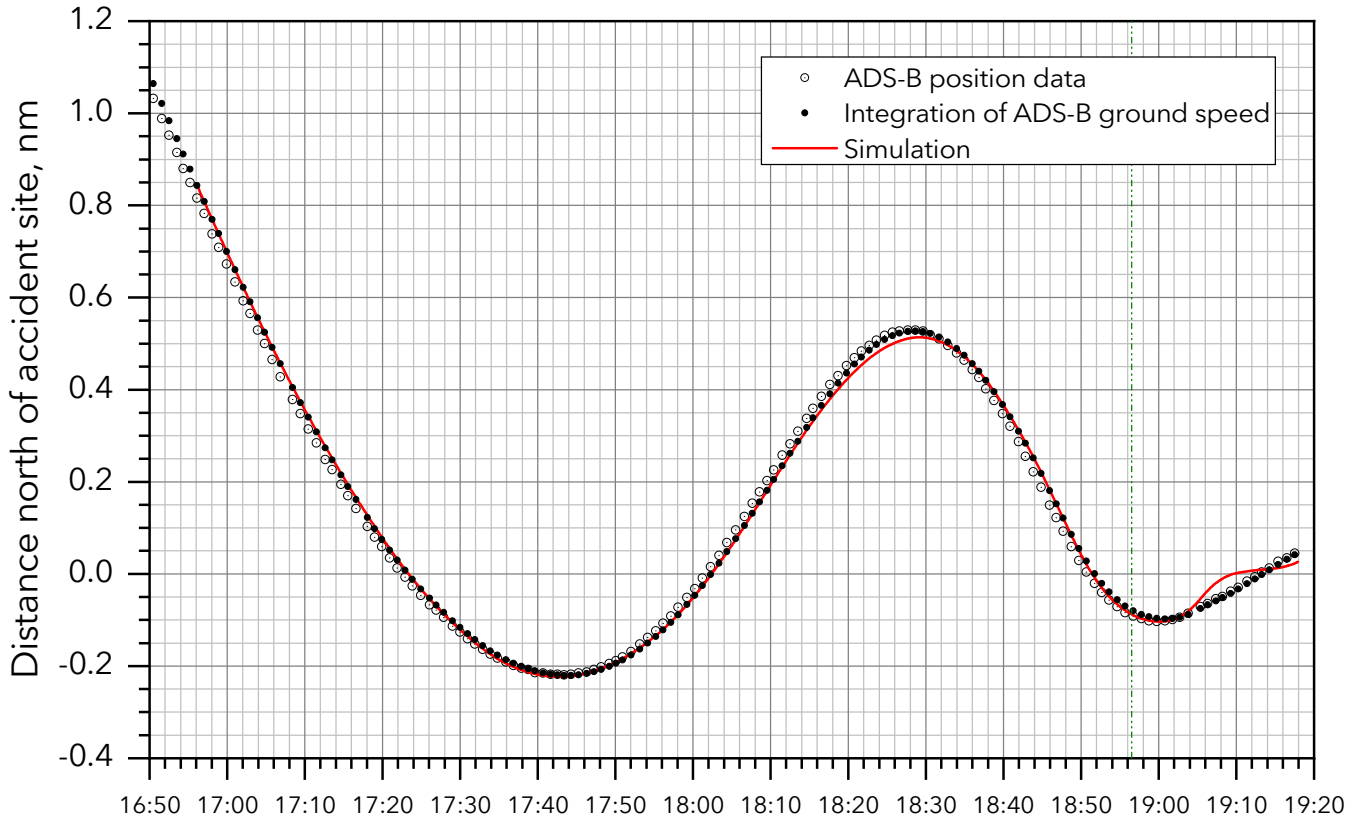
ADS-B time, MM:SS after 10:00:00 PST

AIRCRAFT PERFORMANCE & SIMULATION STUDY

Figure 8a.

WPR23FA034: Cessna 208B, N2069B, Snohomish, WA, 11/18/2022

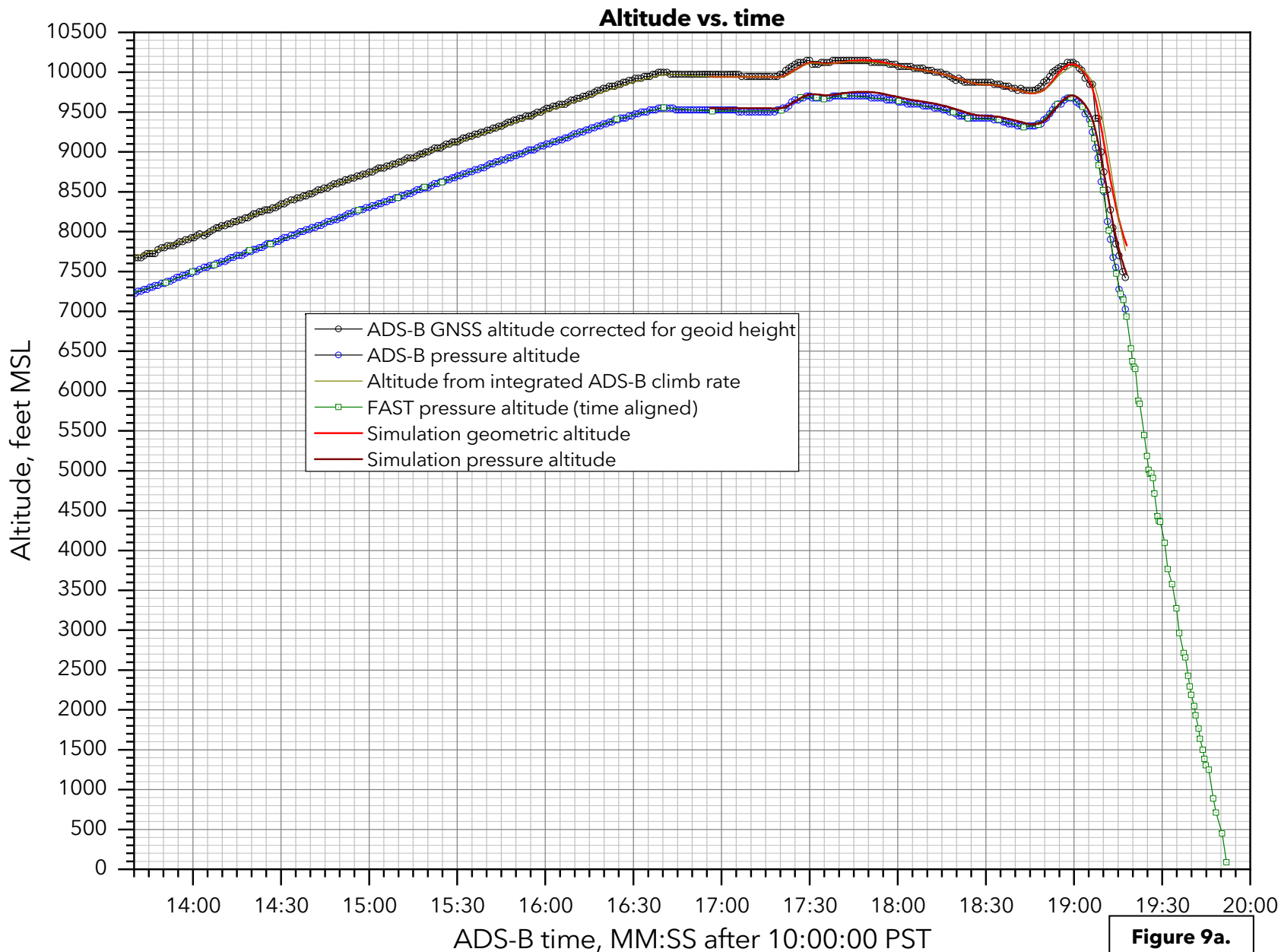
North & east coordinates vs. time (detail)



ADS-B time, MM:SS after 10:00:00 PST

Figure 8b.

WPR23FA034: Cessna 208B, N2069B, Snohomish, WA, 11/18/2022



WPR23FA034: Cessna 208B, N2069B, Snohomish, WA, 11/18/2022

Altitude vs. time (detail)

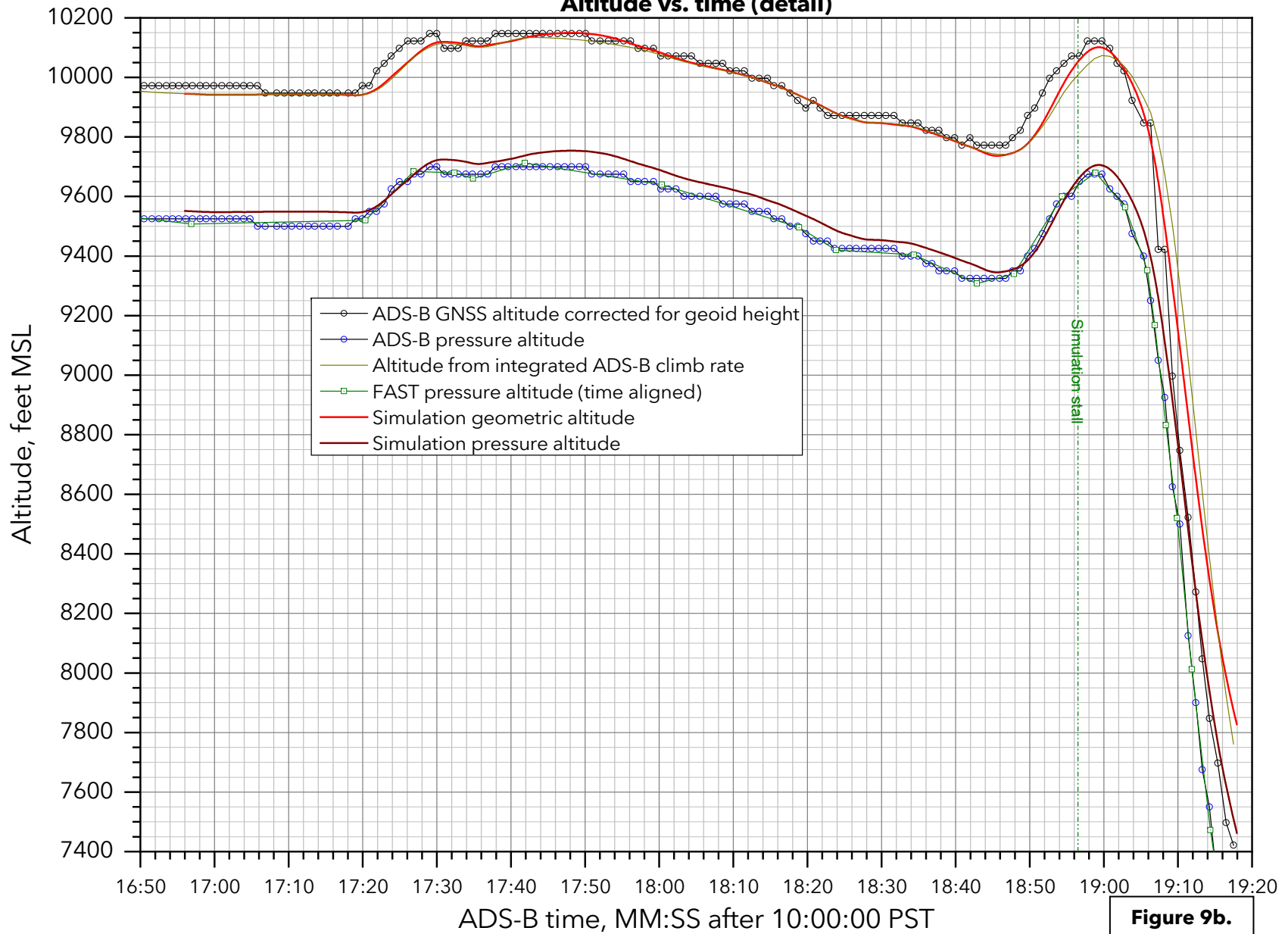


Figure 9b.

WPR23FA034: Cessna 208B, N2069B, Snohomish, WA, 11/18/2022

Altitude vs. time (final descent)

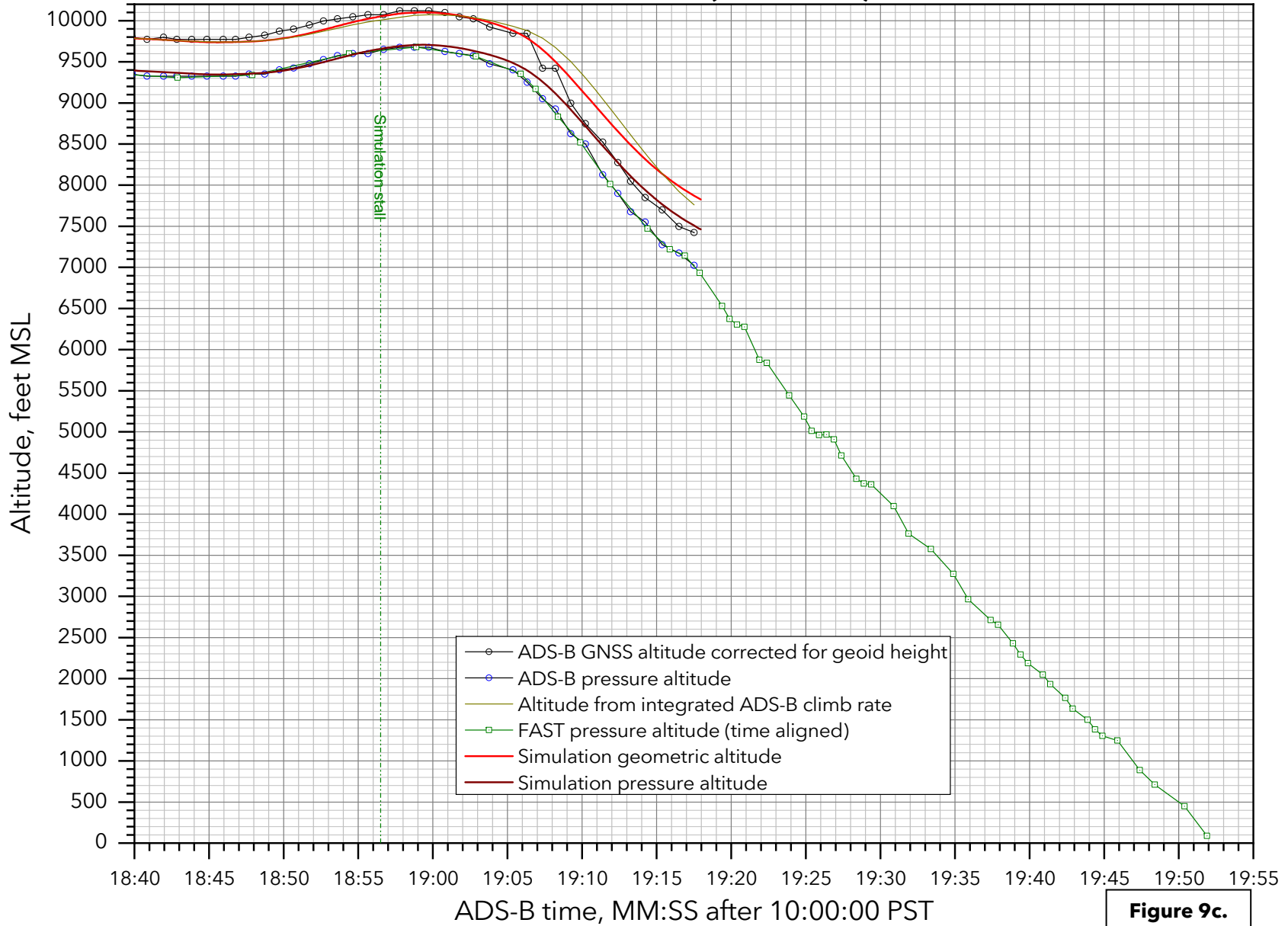
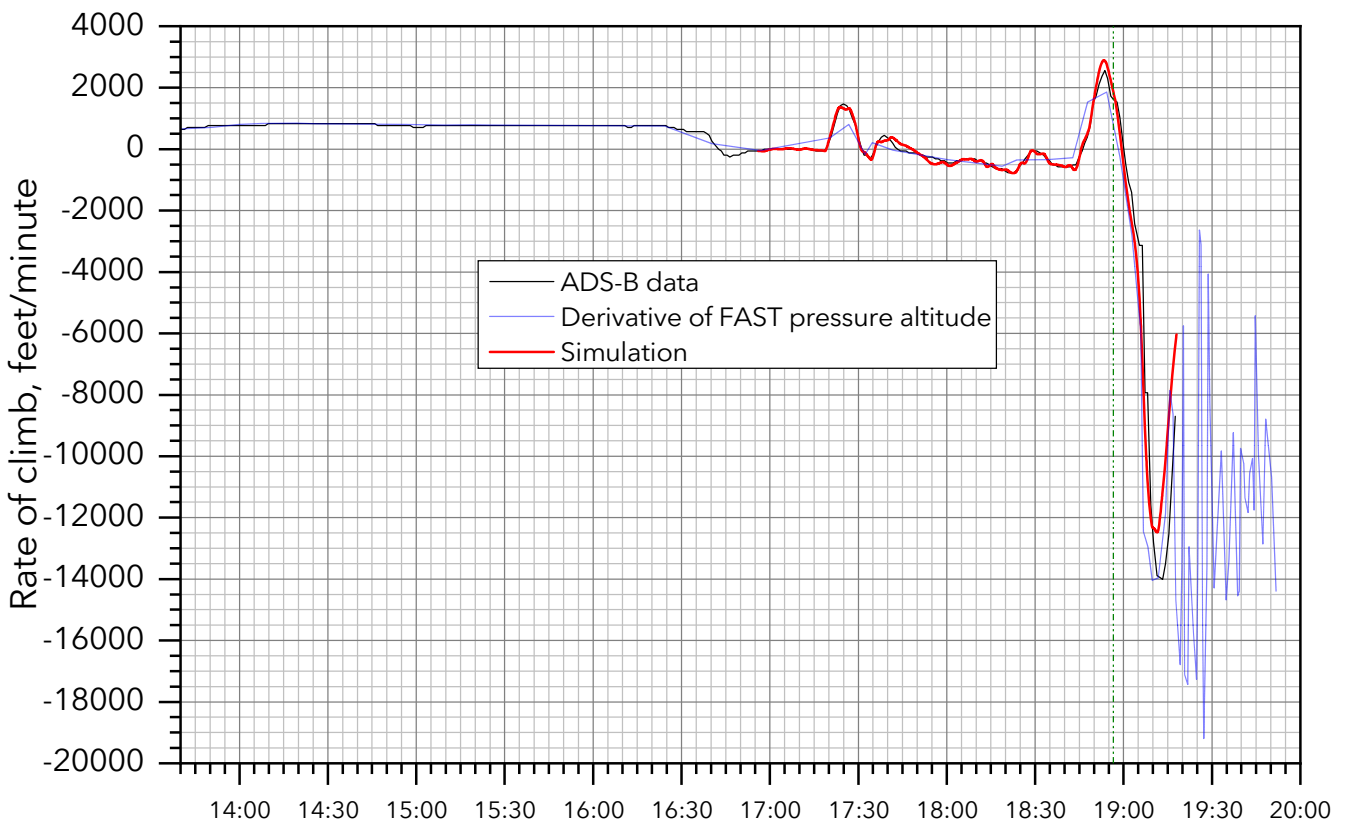
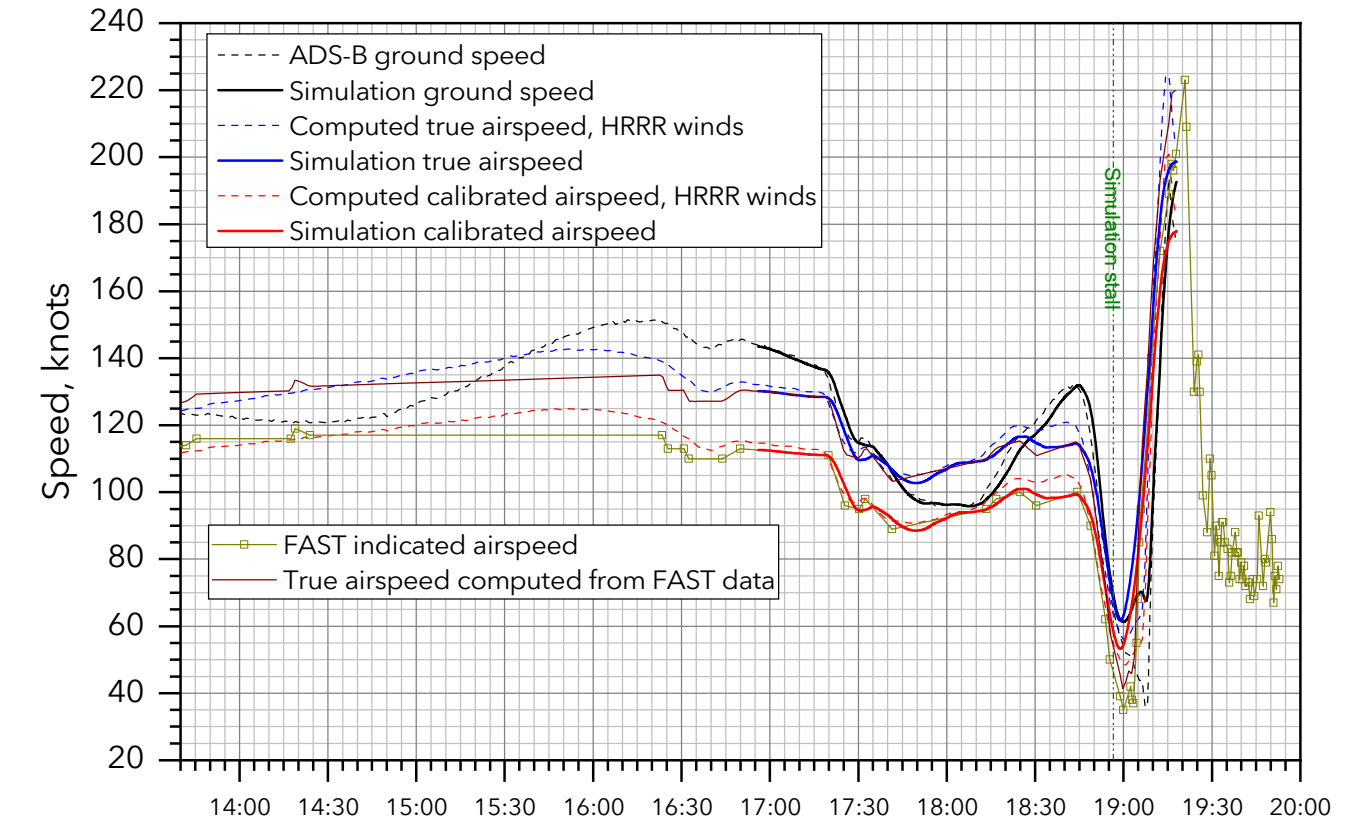


Figure 9c.

WPR23FA034: Cessna 208B, N2069B, Snohomish, WA, 11/18/2022

Speeds and rate of climb vs. time

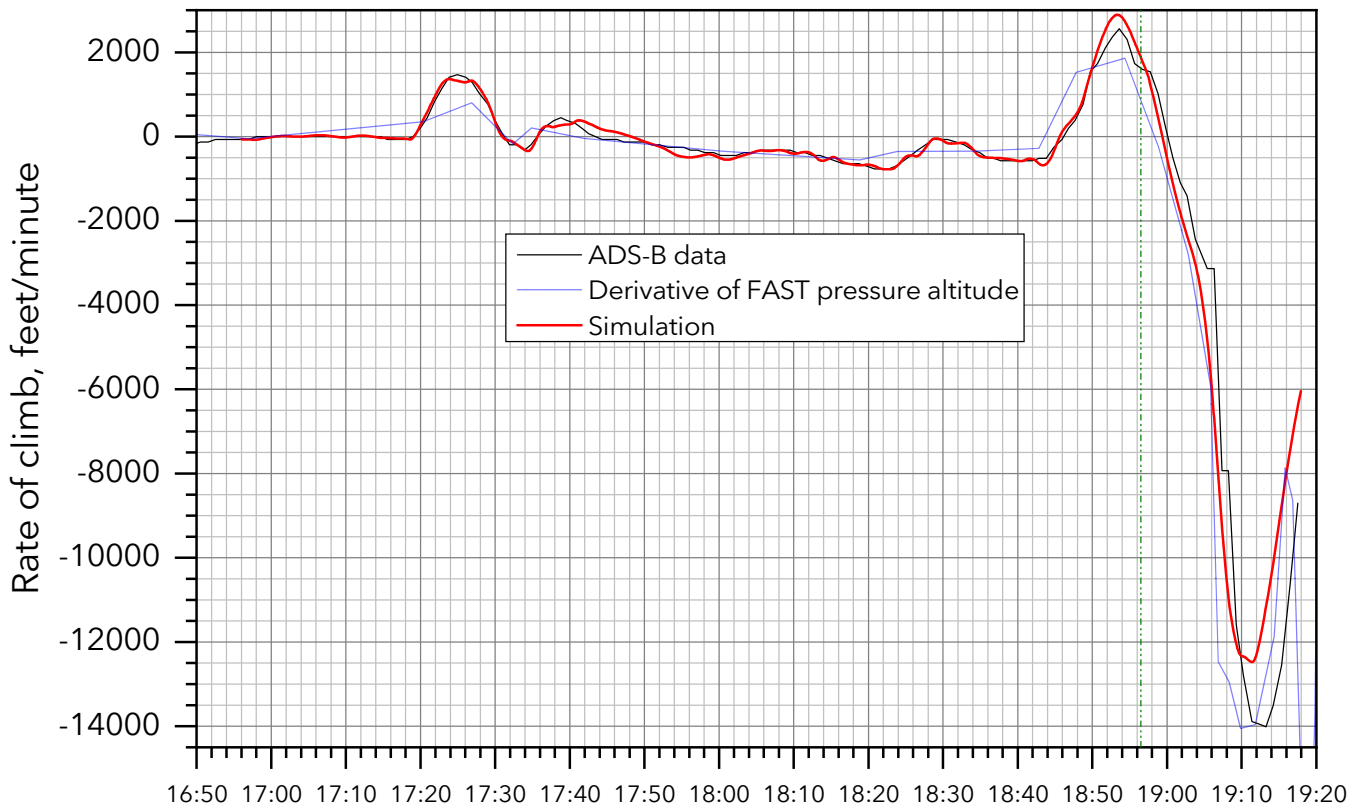
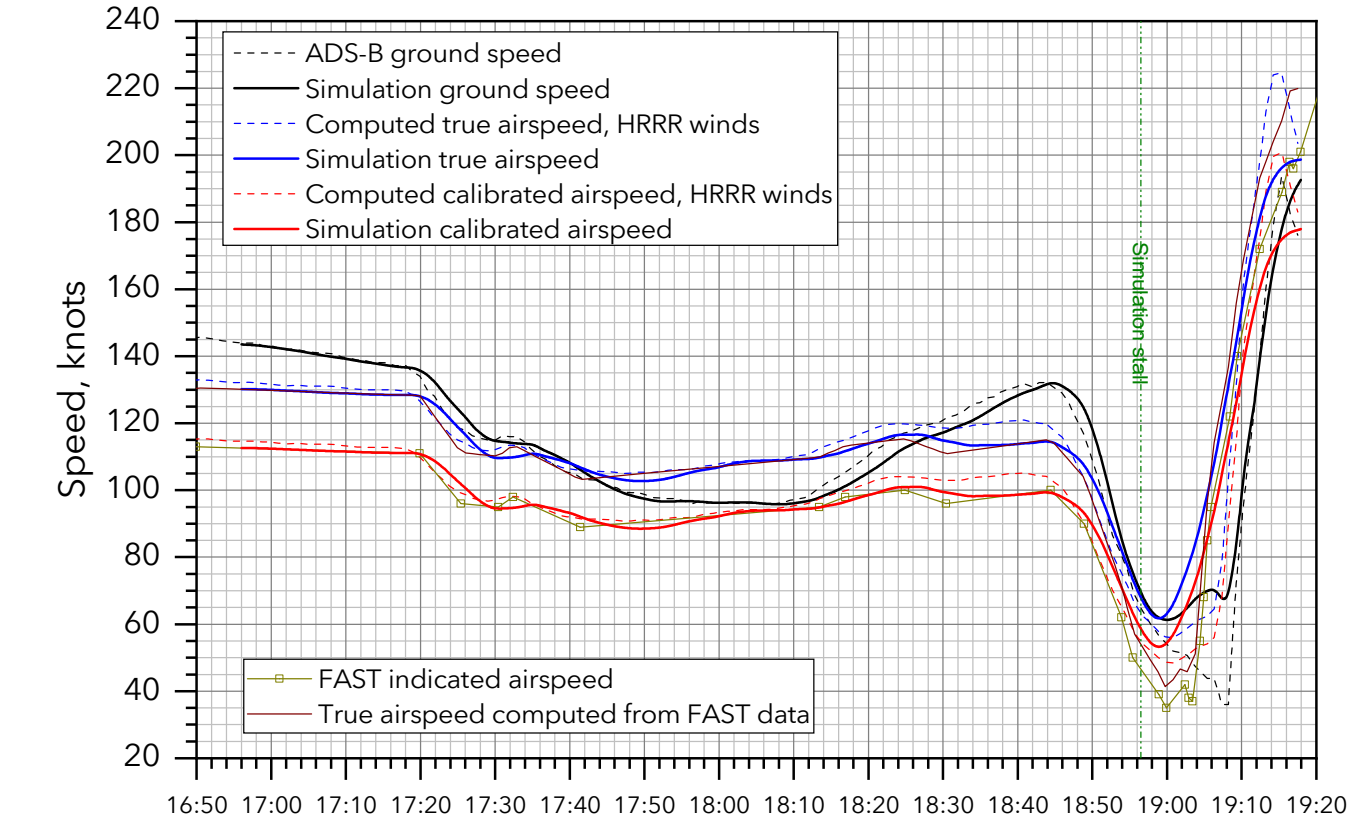


ADS-B time, MM:SS after 10:00:00 PST

Figure 10a.

WPR23FA034: Cessna 208B, N2069B, Snohomish, WA, 11/18/2022

Speeds and rate of climb vs. time (detail)

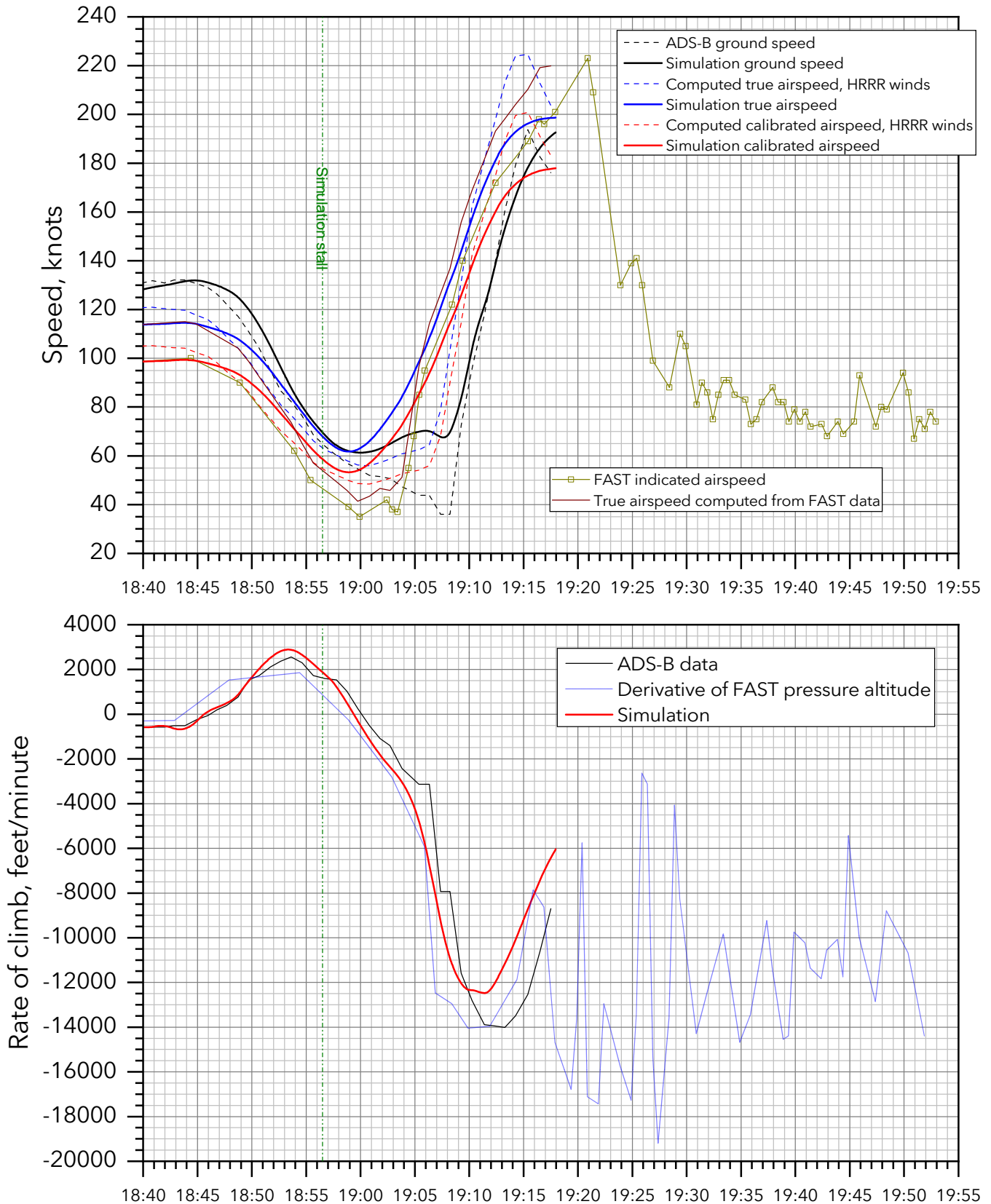


ADS-B time, MM:SS after 10:00:00 PST

Figure 10b.

WPR23FA034: Cessna 208B, N2069B, Snohomish, WA, 11/18/2022

Speeds and rate of climb vs. time (final descent)



ADS-B time, MM:SS after 10:00:00 PST

Figure 10c.

WPR23FA034: Cessna 208B, N2069B, Snohomish, WA, 11/18/2022

Euler angles vs. time

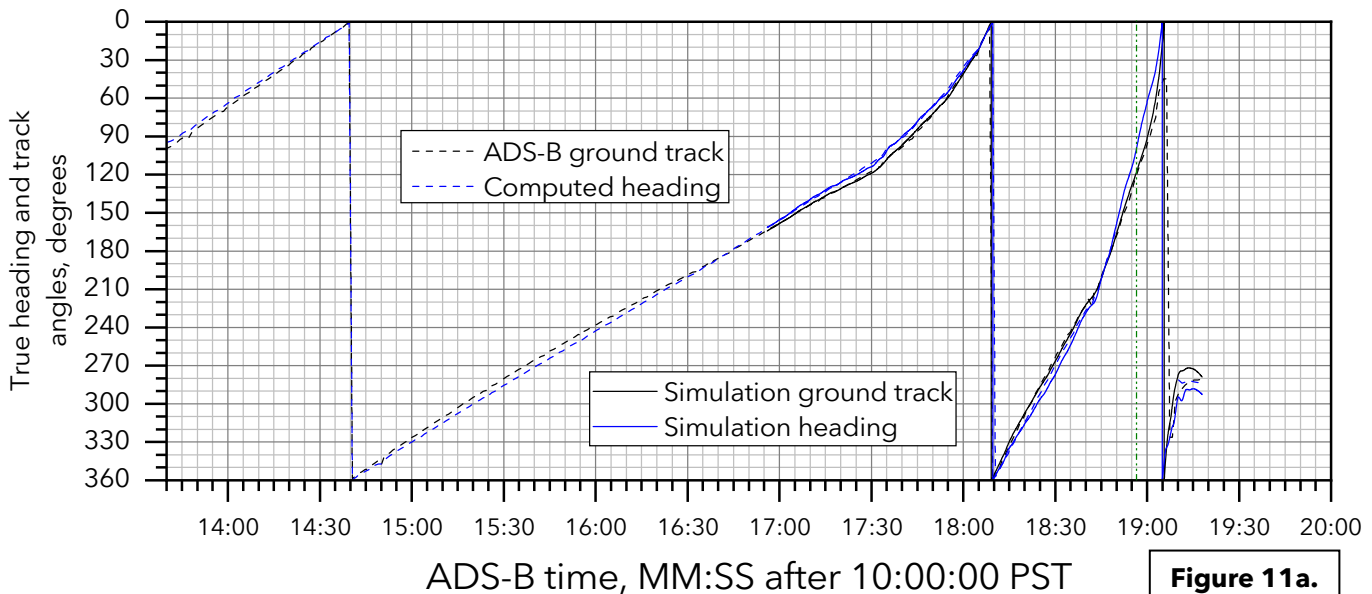
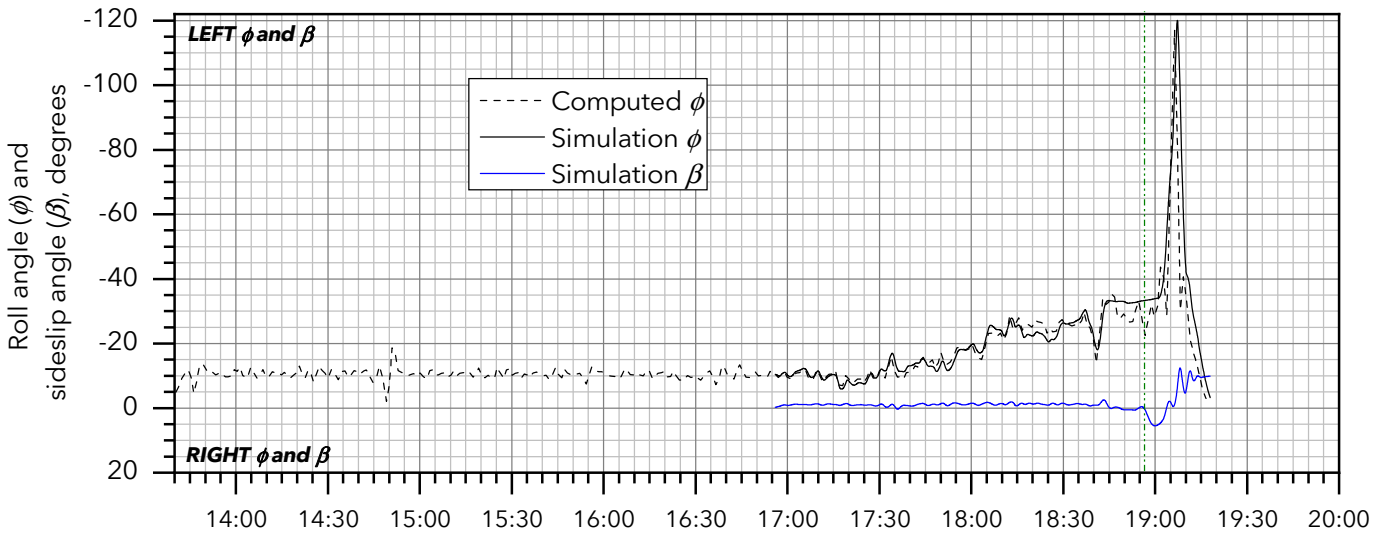
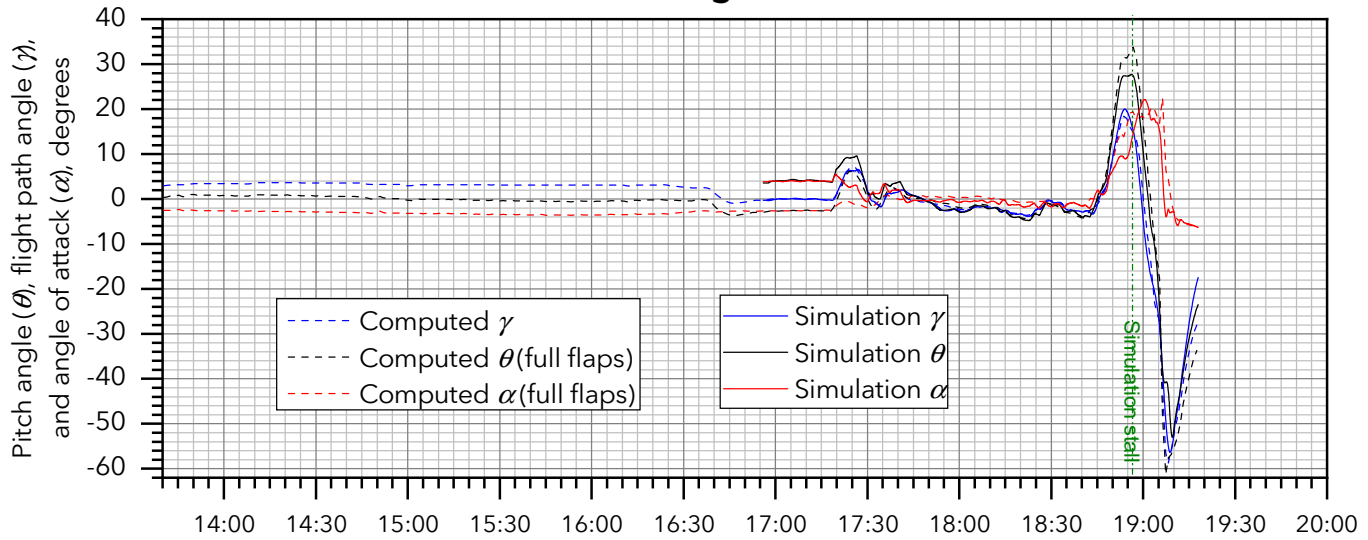
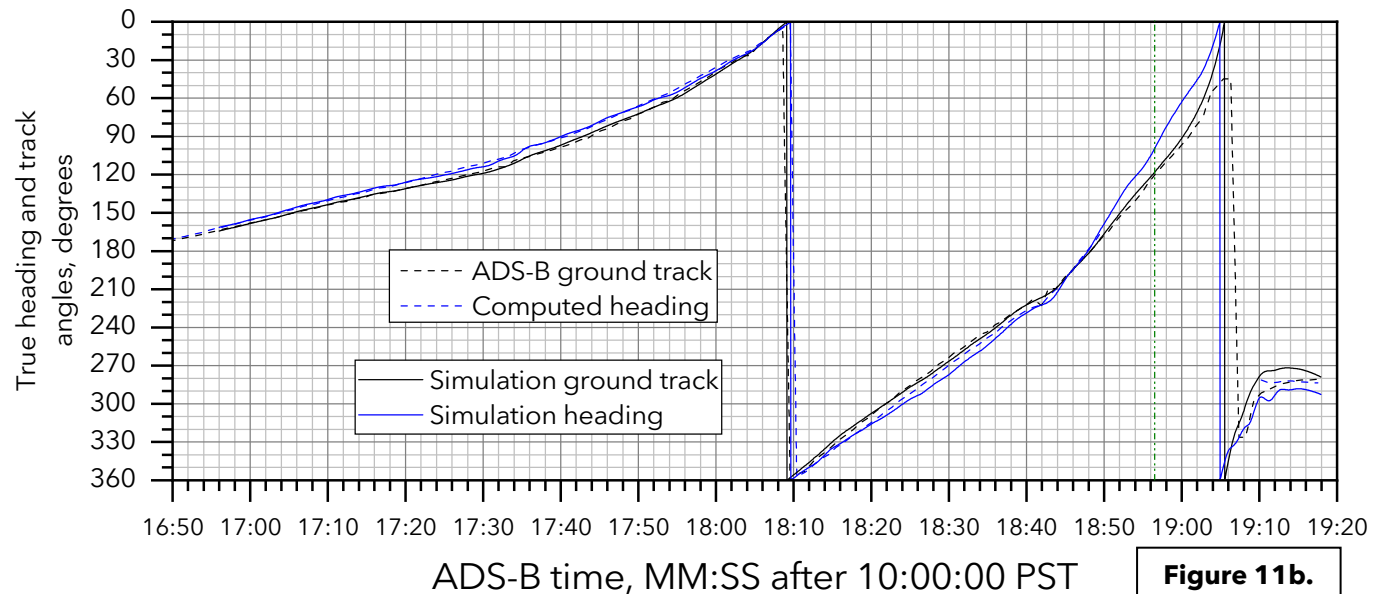
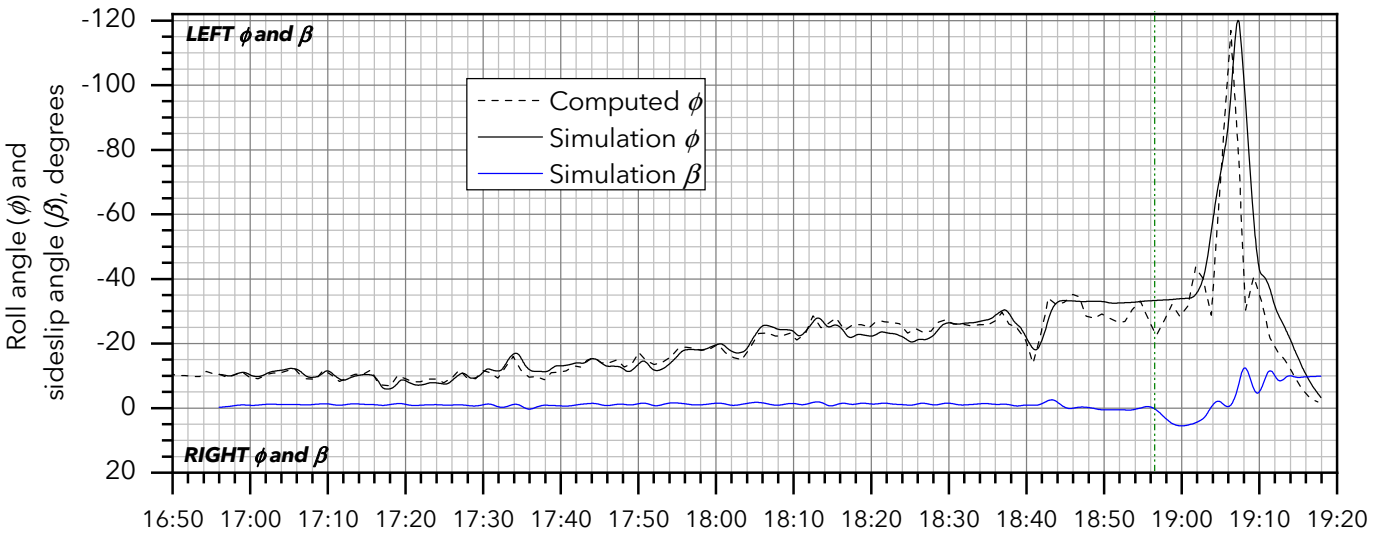
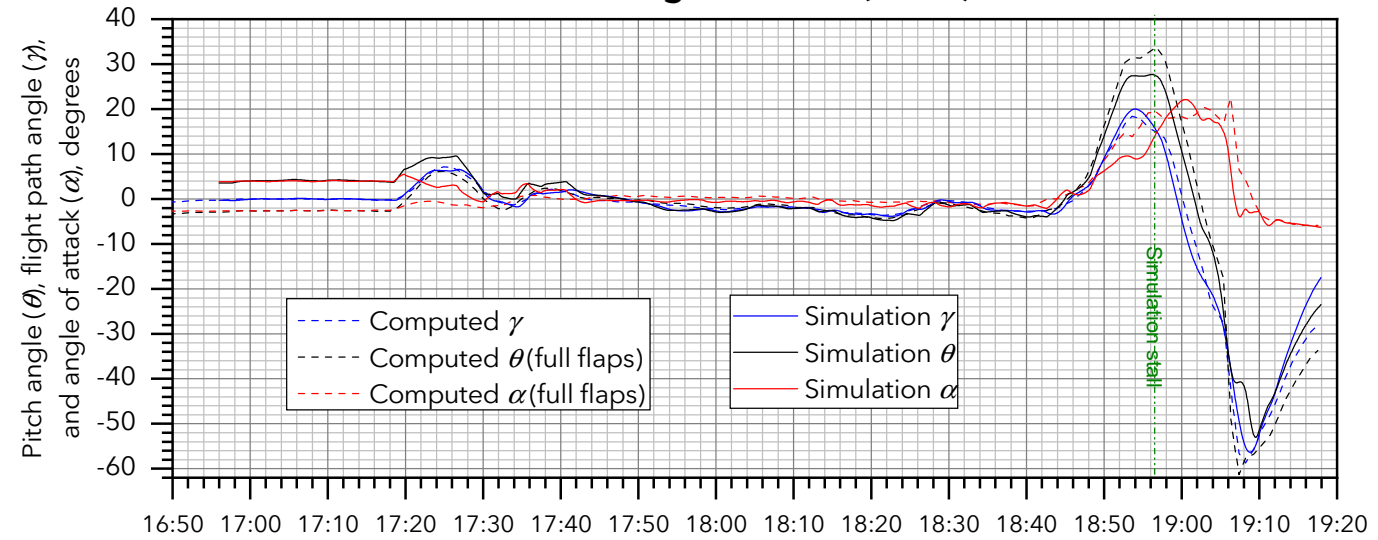


Figure 11a.

WPR23FA034: Cessna 208B, N2069B, Snohomish, WA, 11/18/2022

Euler angles vs. time (detail)



ADS-B time, MM:SS after 10:00:00 PST

Figure 11b.

WPR23FA034: Cessna 208B, N2069B, Snohomish, WA, 11/18/2022

Load factors vs. time

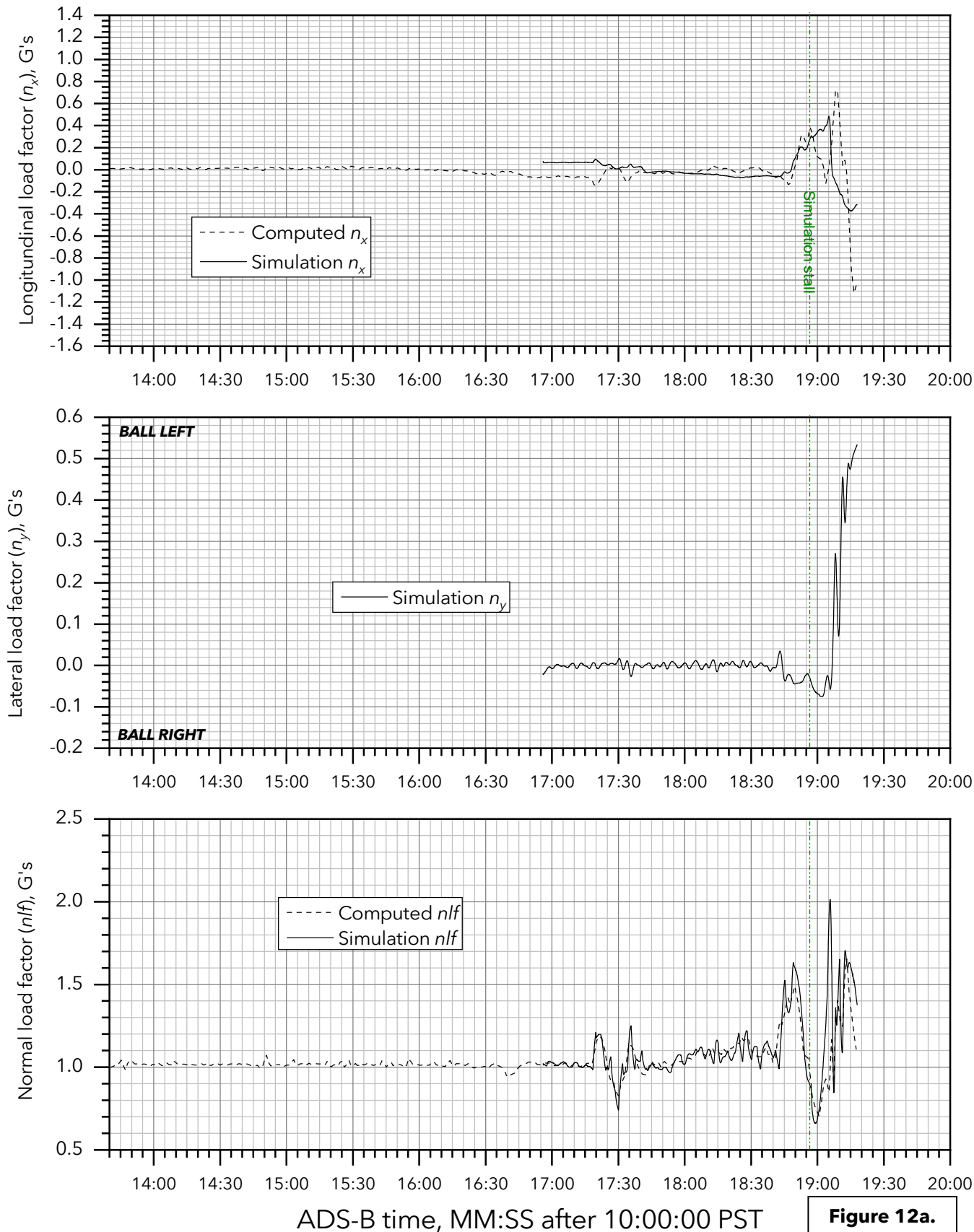
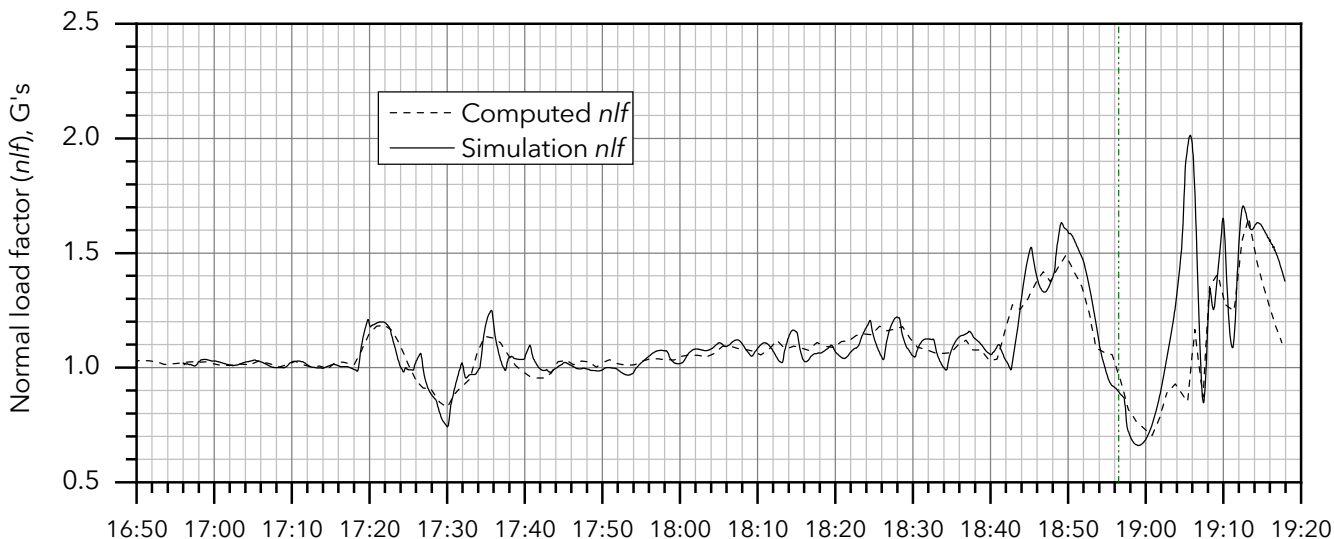
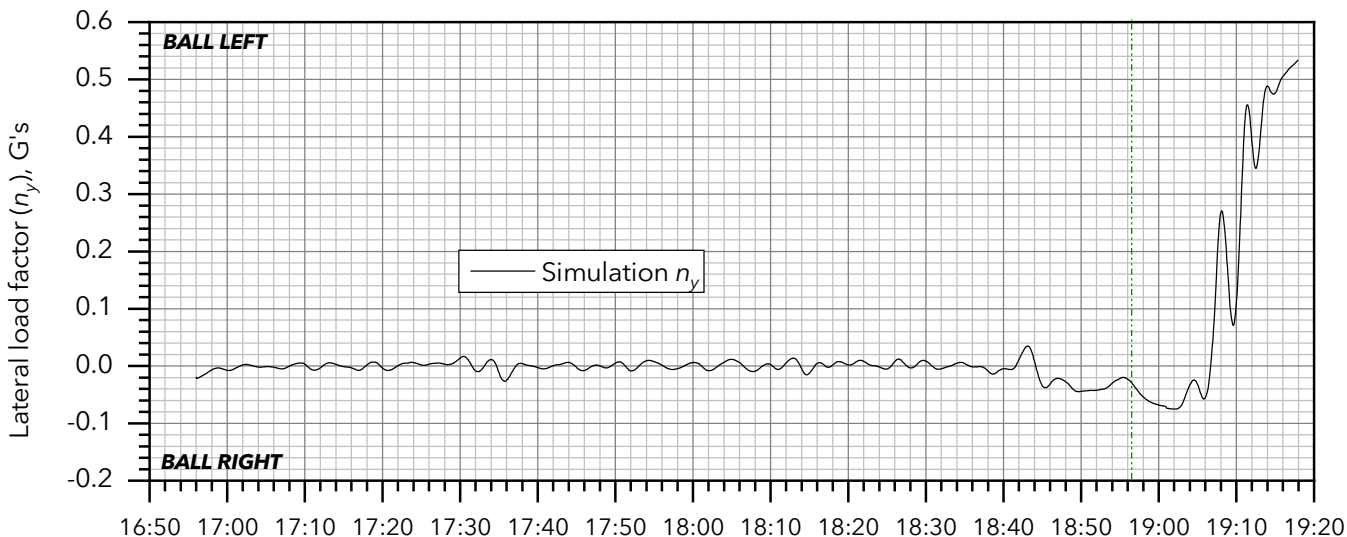
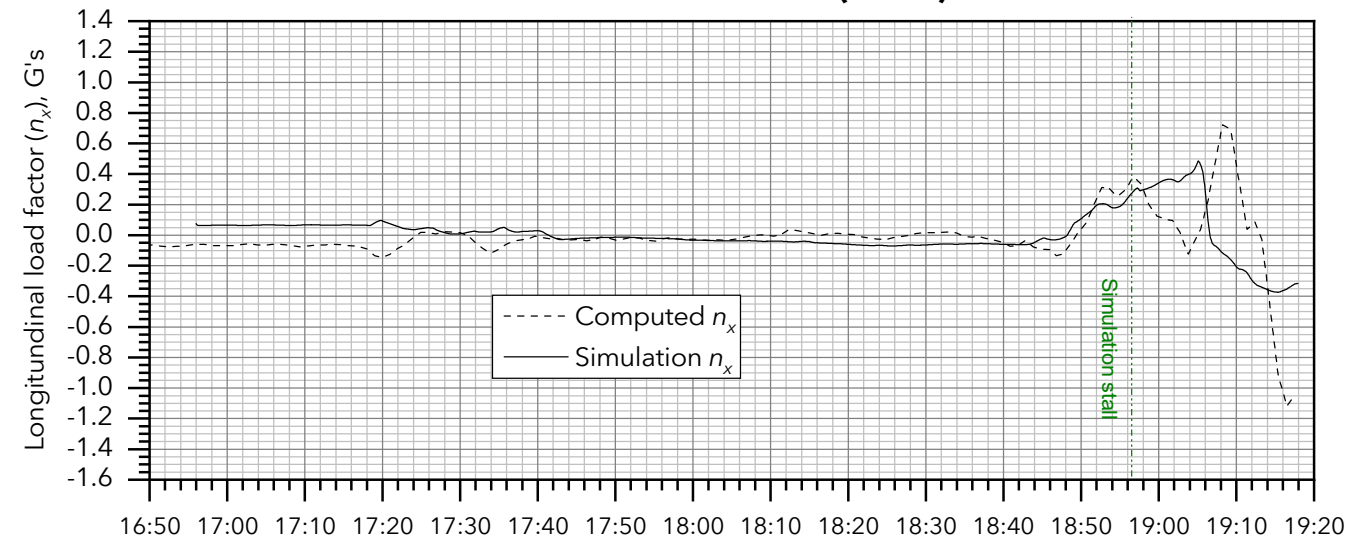


Figure 12a.

WPR23FA034: Cessna 208B, N2069B, Snohomish, WA, 11/18/2022

Load factors vs. time (detail)



ADS-B time, MM:SS after 10:00:00 PST

Figure 12b.

WPR23FA034: Cessna 208B, N2069B, Snohomish, WA, 11/18/2022

Simulation flight controls vs. time

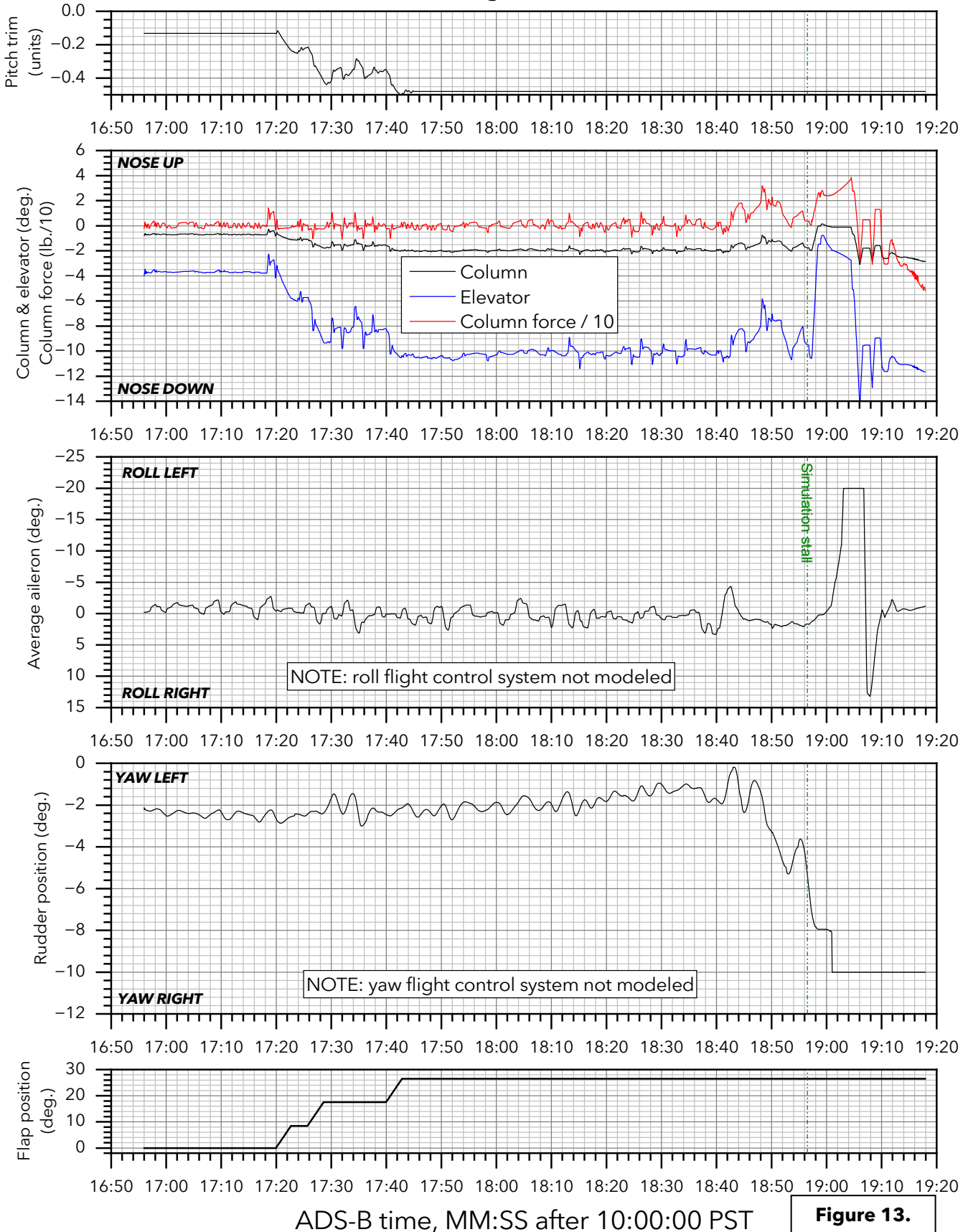


Figure 13.

WPR23FA034: Cessna 208B, N2069B, Snohomish, WA, 11/18/2022

Engine power vs. time

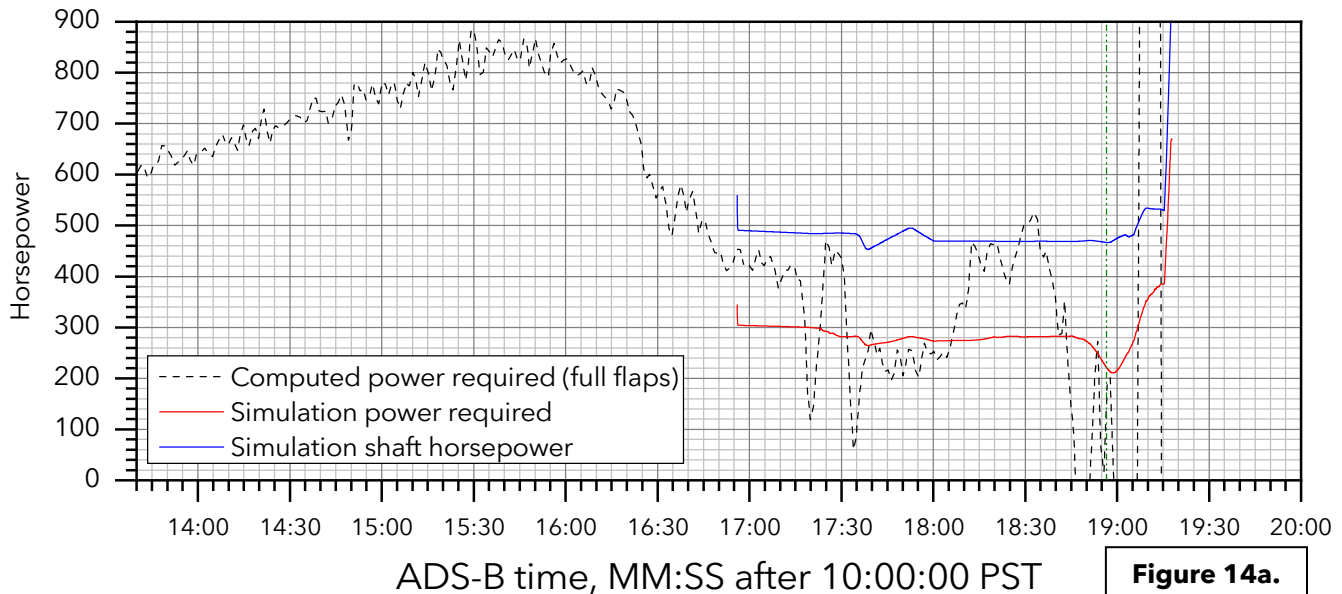
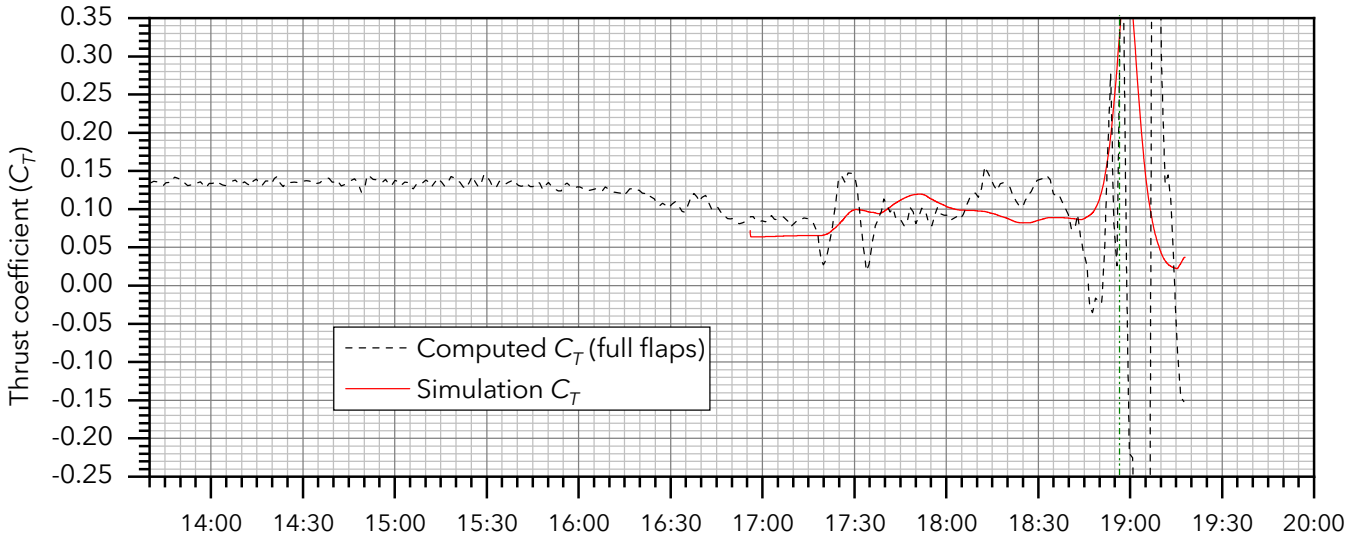
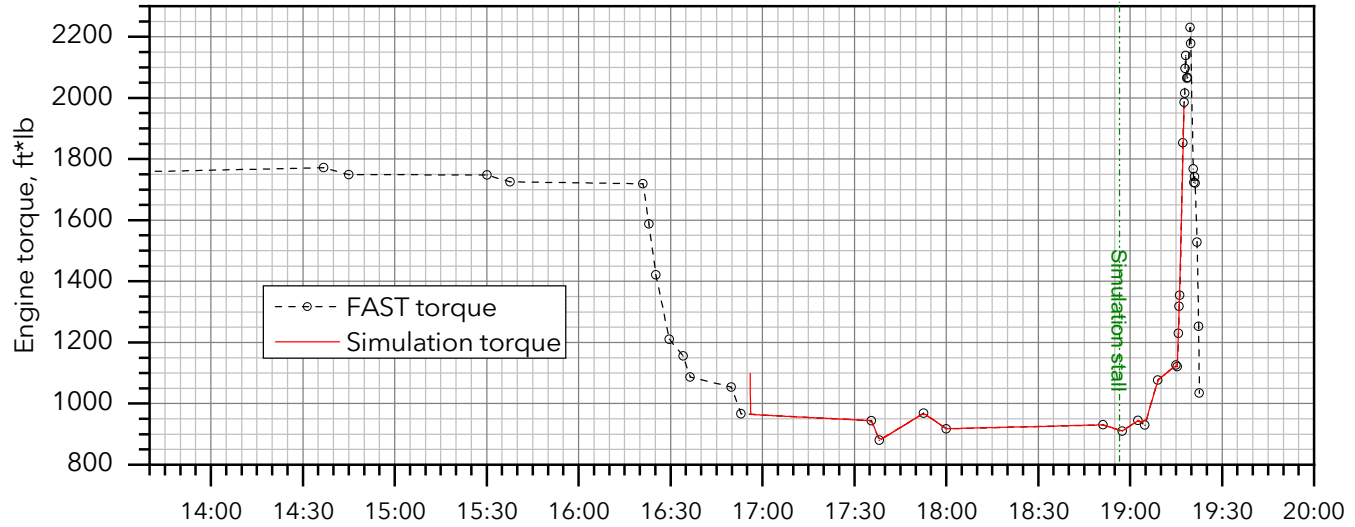


Figure 14a.

WPR23FA034: Cessna 208B, N2069B, Snohomish, WA, 11/18/2022

Engine power vs. time (detail)

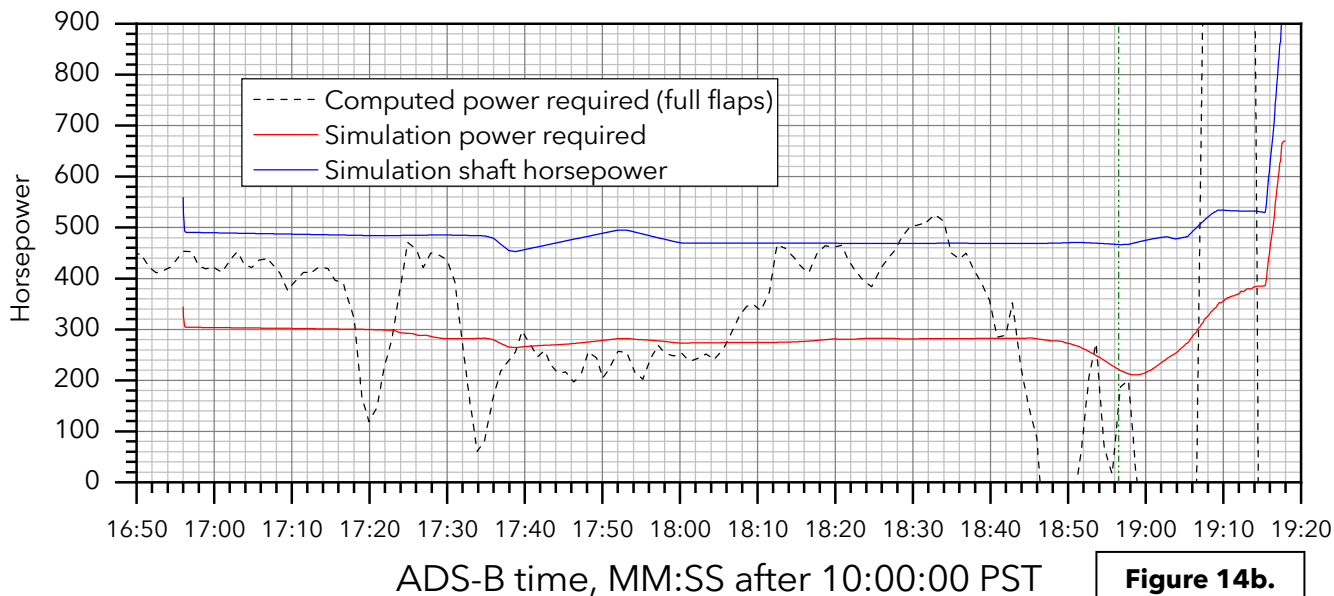
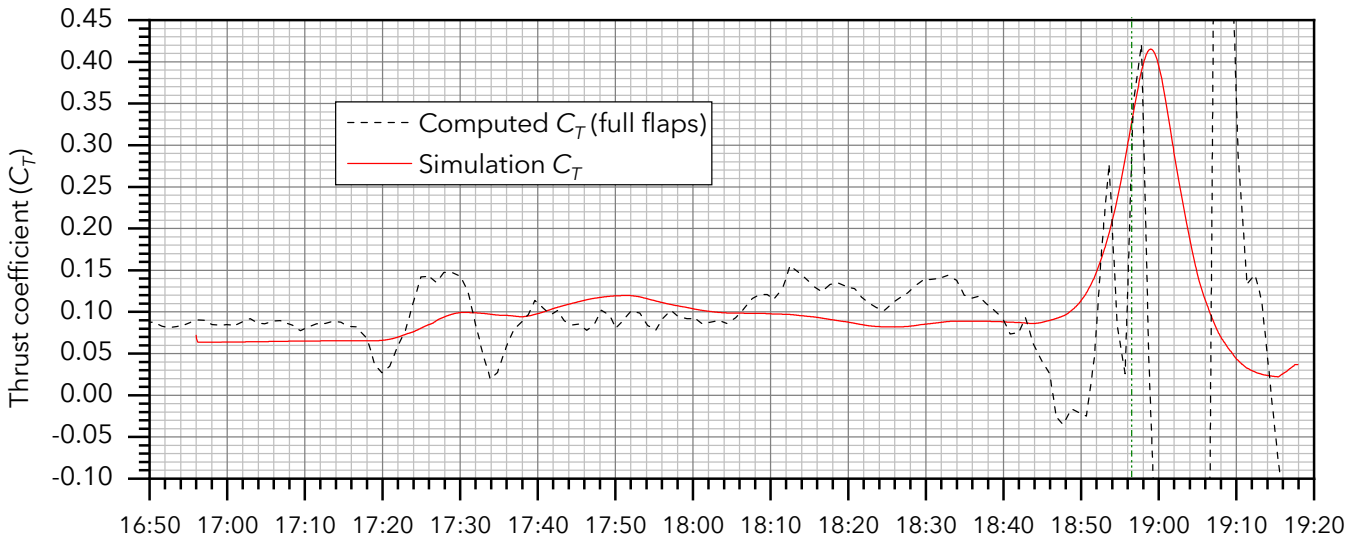
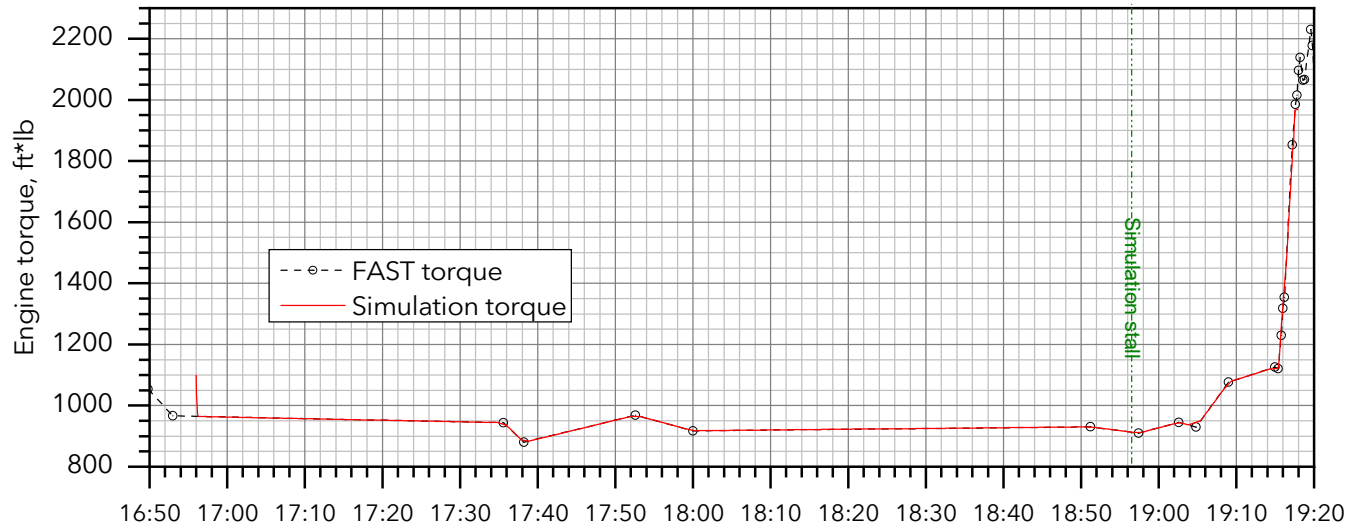
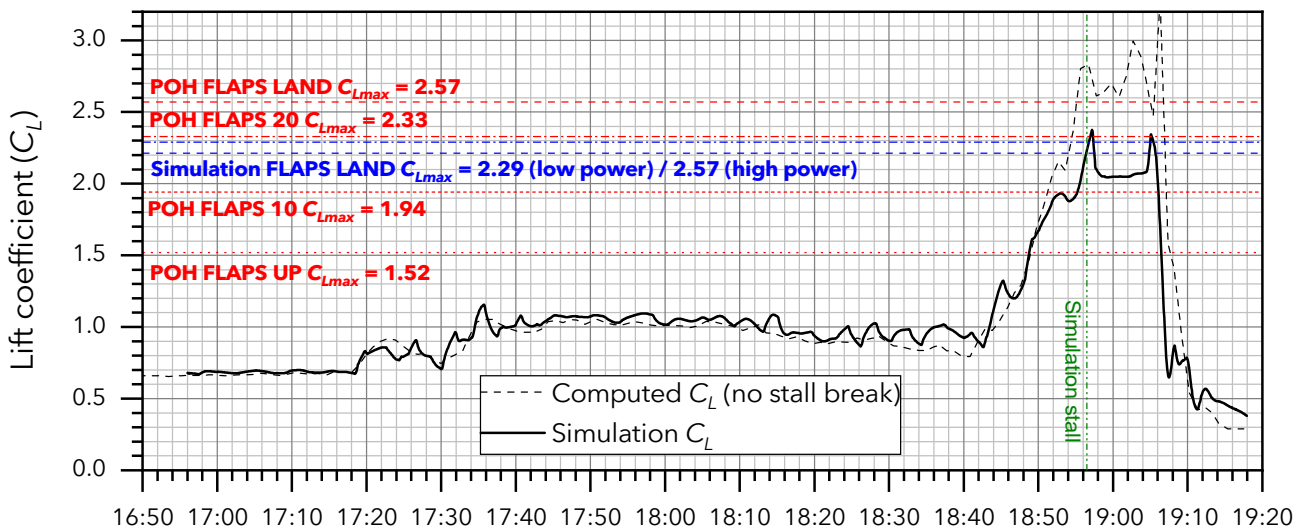
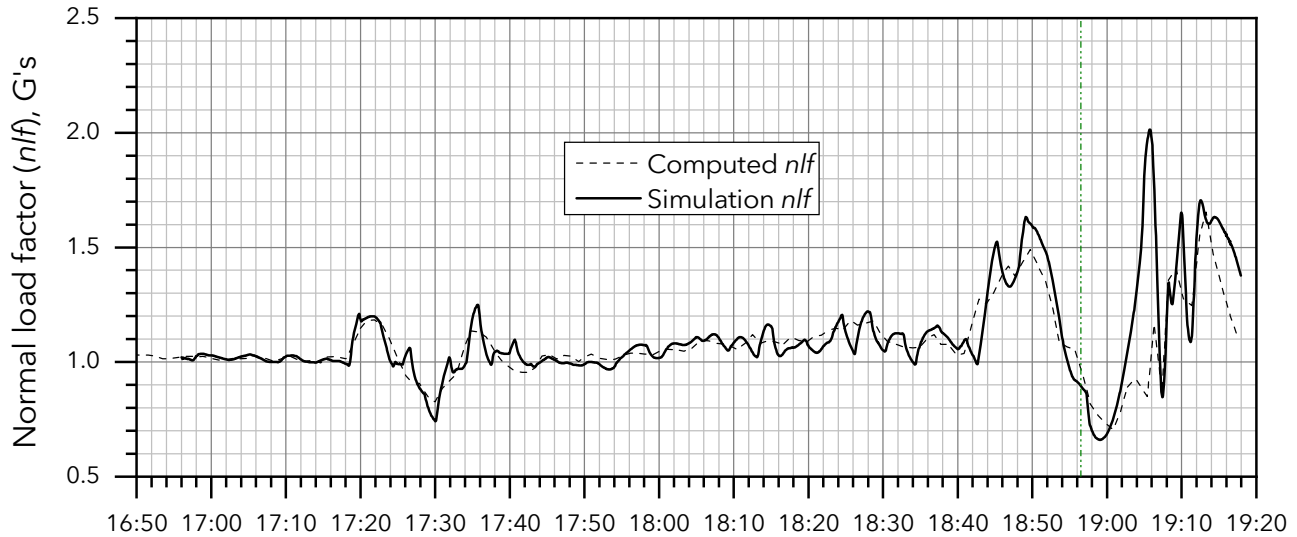
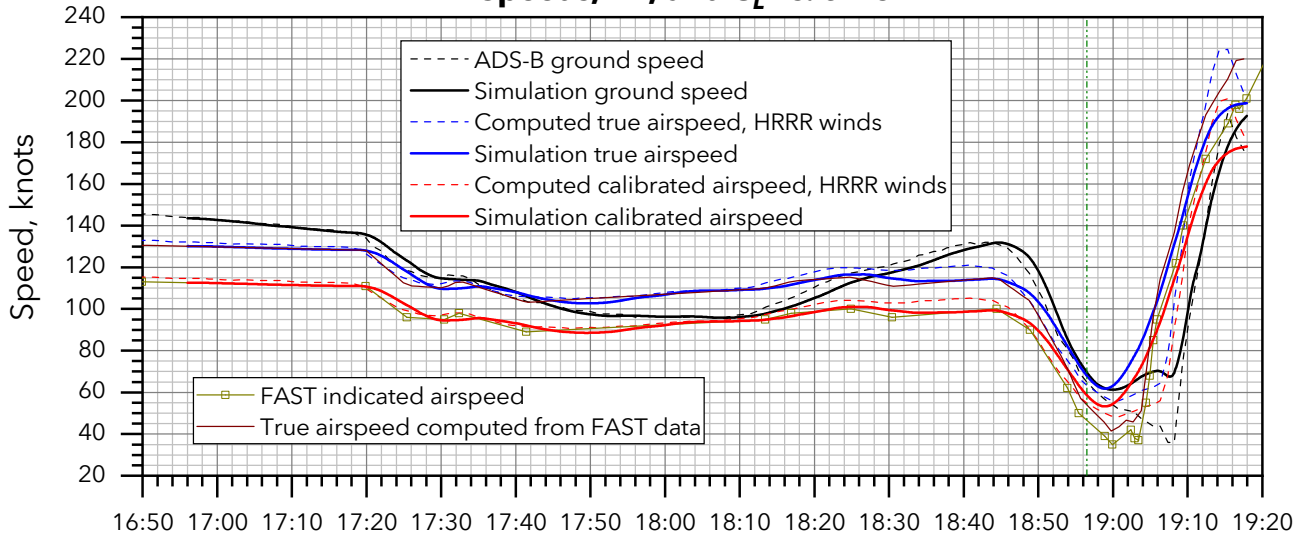


Figure 14b.

WPR23FA034: Cessna 208B, N2069B, Snohomish, WA, 11/18/2022

Speeds, nlf , and C_L vs. time



ADS-B time, MM:SS after 10:00:00 PST

Figure 15.

WPR23FA034: Cessna 208B, N2069B, Snohomish, WA, 11/18/2022

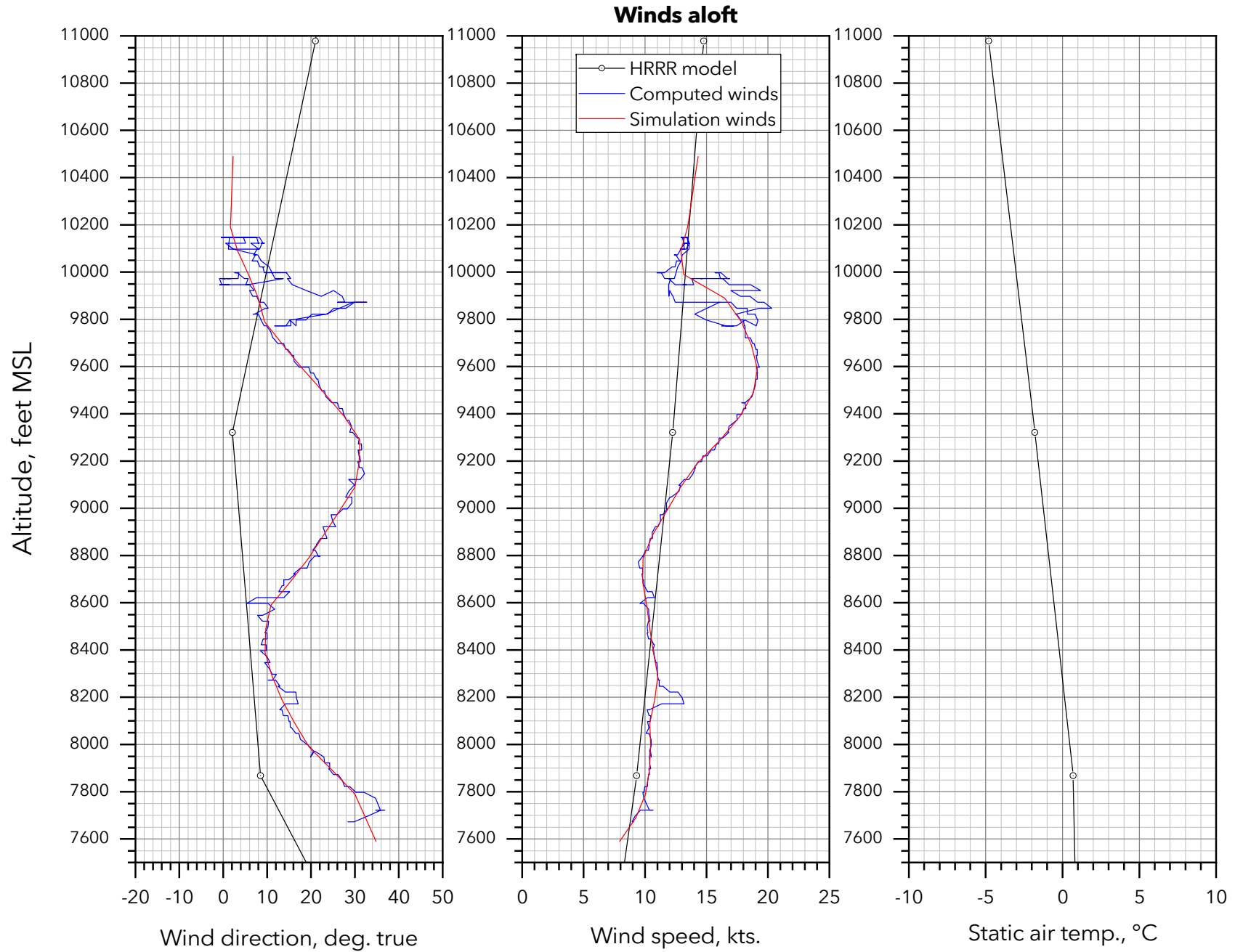




Figure 17a. Video frame from Flight 07 condition 5.6L, showing displacement of the Slip / Skid Indicator bar, and a roll angle greater than 30° just prior to the stall break.



Figure 17b. Video frame from Flight 07 condition 5.6L, showing a roll angle past -60° following the stall break. The PFD was obscured by the pilot's body for a few seconds after the stall, but recorded data indicates that the roll angle reached -83°. Subsequent frames show the pitch angle at about -45°.

Hazard Number: 9.5		Risk Assessment					
Test Type: Aft CG Stall Characteristics	Catastrophic	Avoid	High	High	Medium	Low	
	Hazardous	Avoid	High	Medium	Medium	Low	
Hazard: Deprature from controlled flight	Major	High	High	Medium	Medium	Low	
	Minor	Medium	Medium	Medium	Low	Low	
Cause: Unpredicted aerodynamic response Improper control inputs	No Safety Effect	Low	Low	Low	Low	Low	
	Severity	Frequent	Probable	Occasional	Remote	Improbable	
Effect: Loss of significant amount of altitude which leads to a ground impact	Probability	Frequent	Probable	Occasional	Remote	Improbable	
Mitigations and Minimizing Procedures: 1 Minimum altitude to begin a stall condition 5,000 ft AGL. 2 Conduct test during day VFR in smooth air. 3 Flight crew familiar with stall characteristics and recovery techniques. 4 Flight control rigging confirmed within maintenance manual specifications. 5 Review anticipated stall warning activation speed. 6 Review AFM stall recovery procedures. 7 Recovery to be initiated once stall is reached, and not more than 2 seconds after reaching the aft column stop							
Emergency Procedures: If an unintentional spin is encountered: Retard power to idle position; Place ailerons in neutral position; Apply and HOLD full rudder opposite to the direction of rotation; Immediately after the rudder reaches the stop, move the control wheel BRISKLY forward far enough to break the stall. Full down elevator may be required at aft center of gravity loadings to assure optimum recoveries. HOLD these control inputs until rotation stops. Premature relaxation of the control inputs may extend the recovery. As rotation stops, neutralize rudder and make a smooth recovery from the resulting dive. (Reference AFM, Emergency Procedures Section)							
Weather Requirement and/or Flight Conditions: VFR conditions in smooth air. No flight into known icing.							
Minimum Essential Aircrew: YES NO			Parachutes Required: YES NO				
RISK:	LOW	MEDIUM	HIGH	AVOID			

Prepared by	Date	Title	Document No.
	28 June 2022	Flight Test Plan	22R0112-30-03
Checked by	Date	Aerospace Design & Compliance LLC. 10 Corporate Circle, Suite 225 New Castle, Delaware 19720, USA, email@aerodcllc.com	AC Make
	29 June 2022		Texttron Aviation Inc.
		Page 28 of 28	Rev IR

Figure 18. Test Hazard Analysis for aft-CG stall characteristics testing in the AD&C Flight Test Plan.

Test Hazard Analysis #56

Flight Test Area: Commercial Certification (FAA)

Document Number: 25.203

Document Title: Stall Characteristics

Discipline:

Maneuver Title: Stall

Maneuver Description: As per AC 25-7A Section 6 "Stalls" Para 29

- 1) Trim hands off between 1.13 and 1.3 Vsr1
- 2) 1 kt/sec decel wings level
- 3) 1 and 3 kt/sec turning
- 4) Power off and power on;
- 5) Power on = PLF at MLGW and 1.5 Vsr1, flaps approach
- 6) Stall defined by nose down pitch not readily arrested; deterrent buffet; stick pusher; or stick at the aft stop (2 sec min)

Hazard: Loss of Control

Aircraft Type(s):

Power Plant(s):

Habitation: Inhabited Aircraft Only

Risk Level: High

Risk Criteria:

Corrective Action:

Cause(s):

- Cause #1:**
1. Unpredicted aerodynamic response.
 2. Stick Pusher fails to prevent aircraft from reaching aerodynamic stall.
 3. Improper control inputs.

Mitigation(s):

- Mitigation # 1.1:**
1. Do stall testing in a buildup approach:
 - a. from least risk to highest risk
 - i. forward cg, mid cg, aft cg
 - ii. Power off before power on
 - iii. Wings level before turning
 - iv. 1 kt/sec before 3 kt/sec
 - b. terminate buildup if FAR limits on bank angle are exceeded at any point of the buildup
 2. Establish minimum altitudes for:
 - a. entry,
 - b. recovery initiation,
 - c. recovery chute deployment and
 - d. manual bailout.
 3. Perform pre-flight checks of stall warning and stick pusher, as applicable.
 4. Anti-spin chute must be installed, functional and armed. Perform pre-flight and pre-maneuver checks of chute as applicable.
 5. Minimum crew onboard.
 6. Emergency Egress system must be installed and armed. Perform pre-flight and pre-maneuver checks of egress system as applicable.
 7. Crew to wear helmets and parachutes.
 8. Surface winds must be less than xx kts (parachute dependent).
 9. No aggravated input stalls. All stalls will be ball centered.
 10. No asymmetric power stalls.
 11. If departing controlled flight retard throttles to idle and centralize controls.]
 12. Do not add power during recovery until airspeed is increasing above 1.2 Vs.

Figure 19. Test Hazard Analysis for aft-CG stall characteristics testing in the NASA FTSD.



Figure 20. Video frame from Flight 07 showing an airspeed of 183 KIAS, 8 knots above V_{MO} .

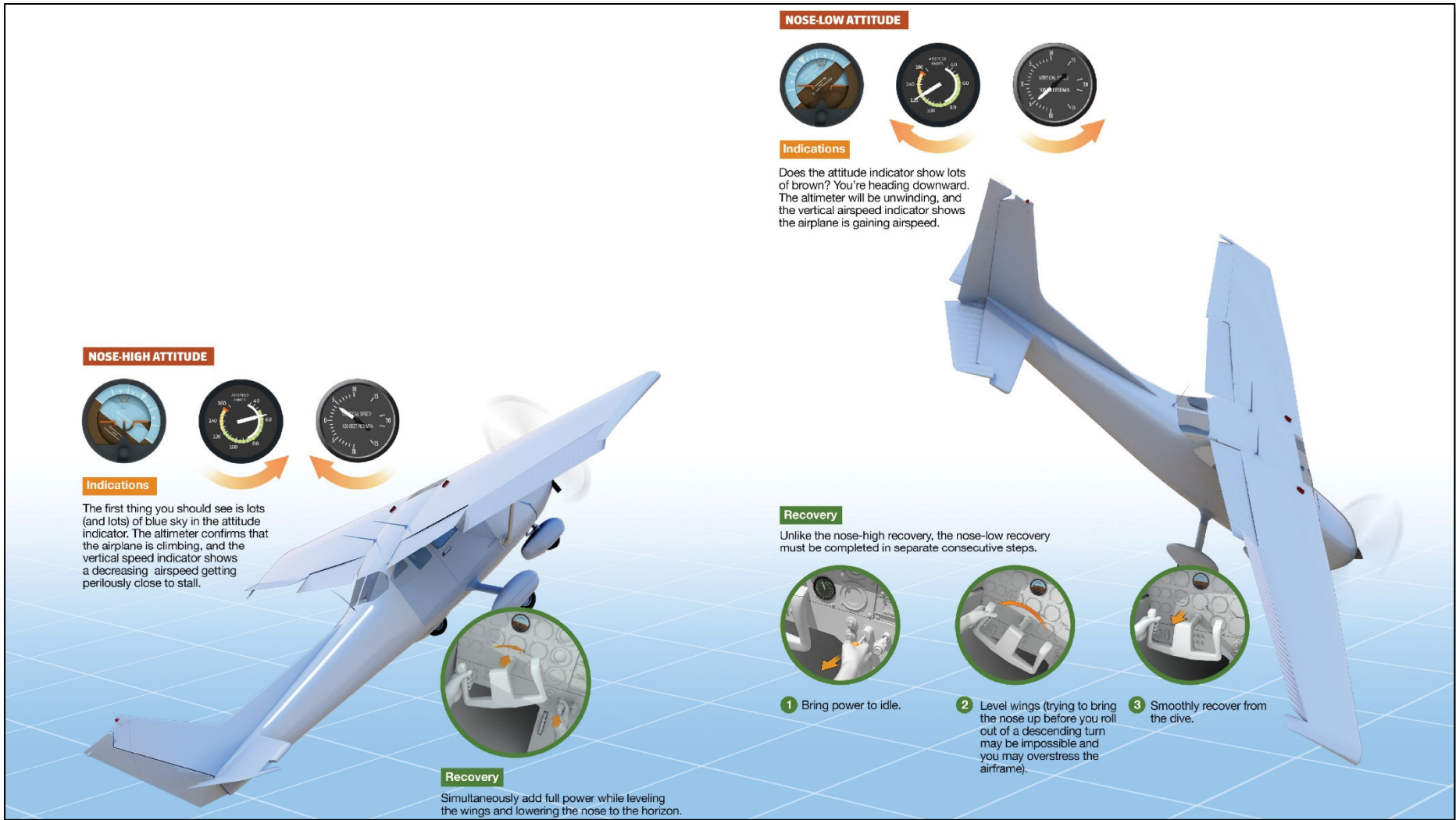
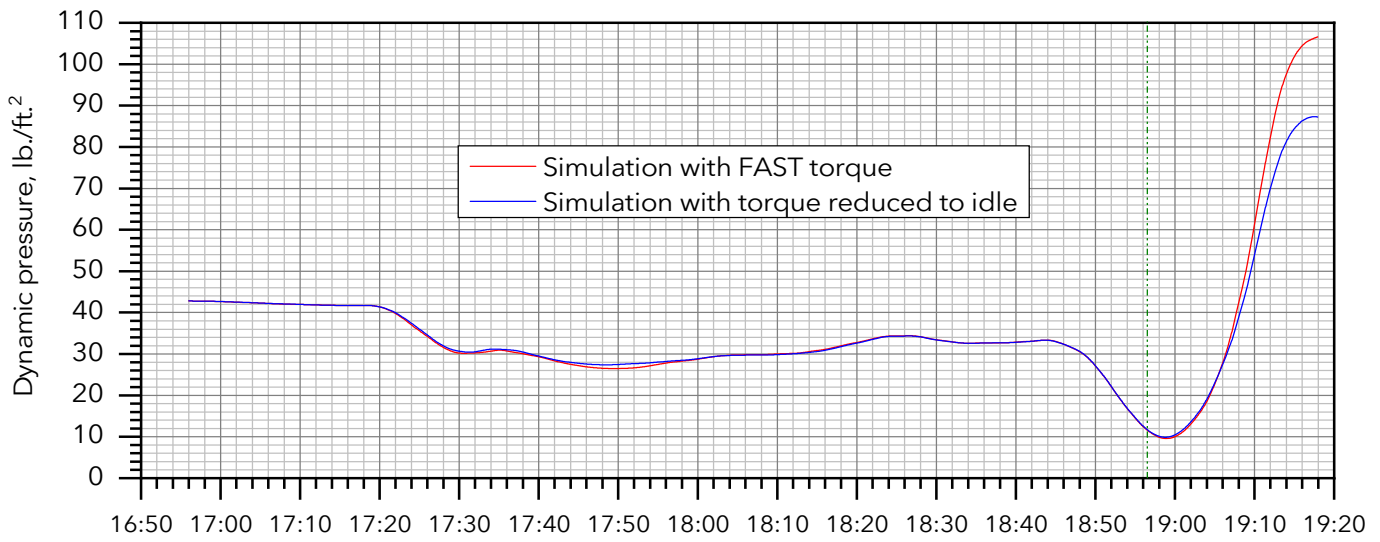
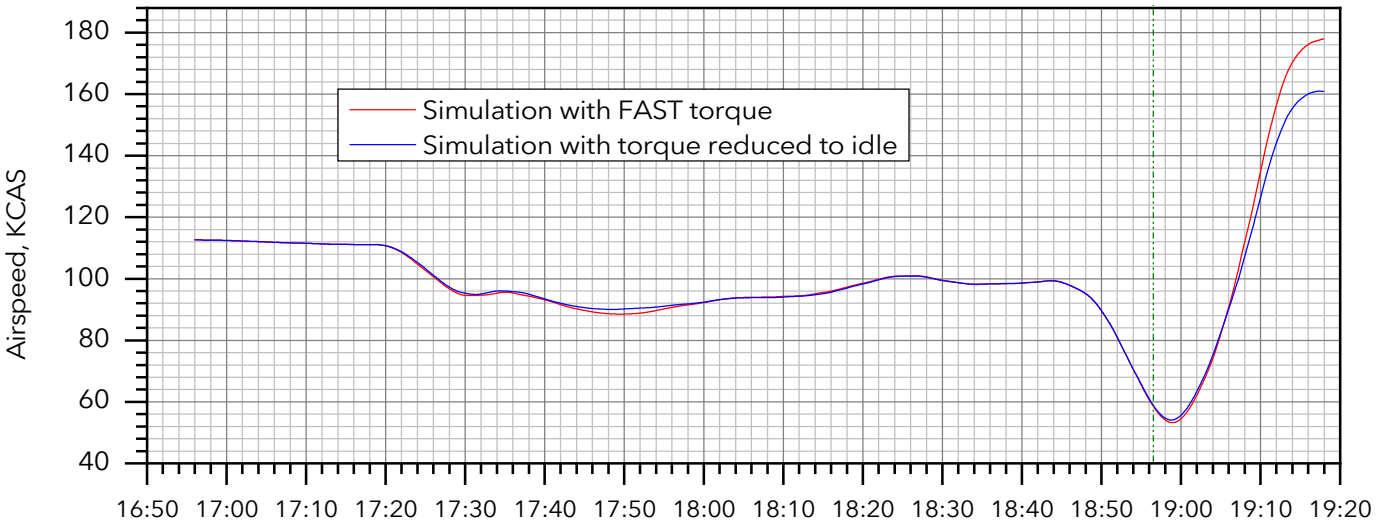
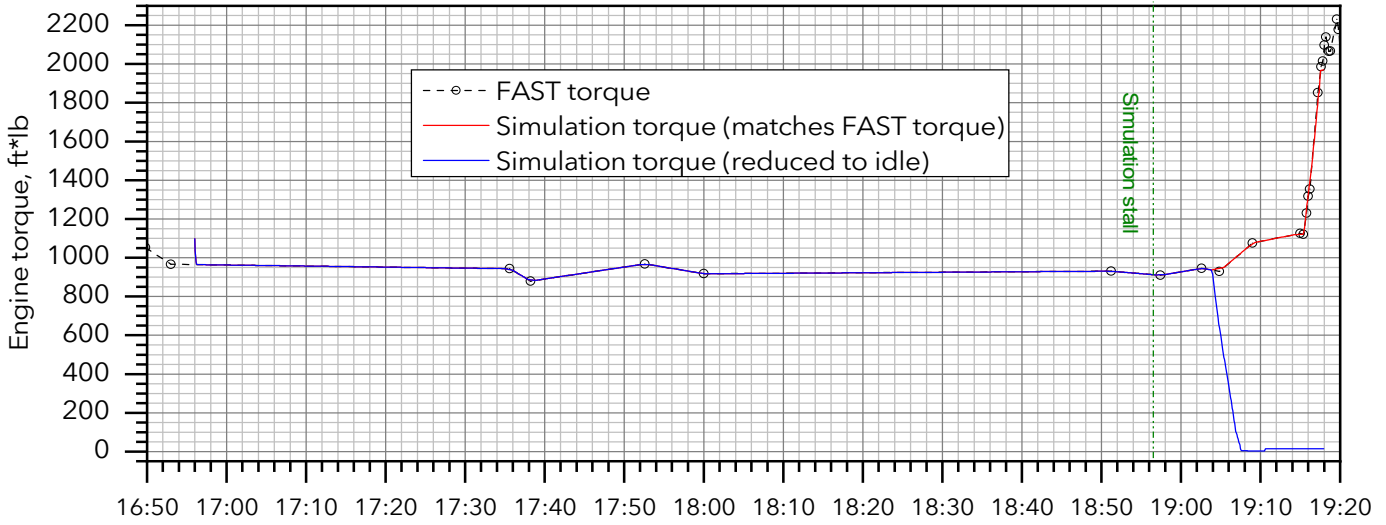


Figure 21. Graphic accompanying AOPA online article regarding unusual attitude recovery.

WPR23FA034: Cessna 208B, N2069B, Snohomish, WA, 11/18/2022

Effect of idle power on post-stall airspeed



ADS-B time, MM:SS after 10:00:00 PST

Figure 22.